Executive Summary

FEEP Microthruster Component Development: Ultraprecise Indium Thruster Contract No. 12376/97/NL/PA – Contract Change Note 4

Prepared by: A. Genovese, W. Steiger, M. Tajmar

Approved by: E. Semerad

Table of Contents

1 INTRODUCTION

1.1 Scope

This executive summary describes the activities carried out within the

FEEP Microthruster Component Development: Ultraprecise Indium Thruster Contract No. 12376/97/NL/PA – Contract Change Note 4

contract. The goal of this contract was split into two different objectives:

- WP 1: 1080 h Endurance test at 75 µN to investigate the wear-out mechanisms
- WP 2: Cluster Test on three ion emitter modules at 75 µN each to investigate ion beam interactions

Regarding workpackage 1, several ion emitter tests have been carried out at 15, 17, 0-25 (profile), 0-35 (profile), 75 and 100 µN. It was soon realised, that the thrust goal of 75 µN was much too high resulting in immediate performance degradation. In total more than 1900 h of accumulated endurance testing was performed at those thrust levels. After in-depth analysis, two wear-out mechanisms have been identified: microdroplet deposition on the extractor as well as erosion of the emitter needle, both depending on the actual thrust level (worse for high thrusts). These results were summarized in a recent ESA-ARCS meeting at Seibersdorf (10.2.2004). The actual endurance test results performed only within the present contract are detailed in Annex A (Status 2001 !).

With respect to workpackage 2, a cluster of three ion emitters has been manufactured. All three of them could be operated together up to 25 µN each. Due to a wetting problem on one of the emitters, only two could be operated together up to the required 75 µN each. Using wire-probe diagnostics, an assessment of beam interactions was carried out. No ion beam interaction could be identified. Numerical simulations were carried out to complement the measurements – also the simulations indicated no ion beam interactions at the separation distances of the used cluster and operating currents. The detailed results are shown in Annex B.

In summary the original objectives (identification of wear-out mechanisms, ion beam interaction at cluster operation) have been met – using tests deviating from the original definitions.

2 ANNEX A – ENDURANCE TESTING

2.1 Characterization Testing

2.1.1 V3G ION EMITTER

The Indium ion emitter (LMS220) flying now on board of CLUSTER II has a small Indium reservoir of about 220 mg, sufficient for S/C potential control (10 to 15 µA), but too small for a thruster (up to 800 µA). In 1997, this reservoir was enlarged to hold 1.2 g of Indium in order to carry out long term tests at high ion currents. **Fig. 1** shows this bigger emitter, LMS1200, both full and empty after life-time testing. Note that the Indium supply was used up to about 99% at the end of the test run.[2]

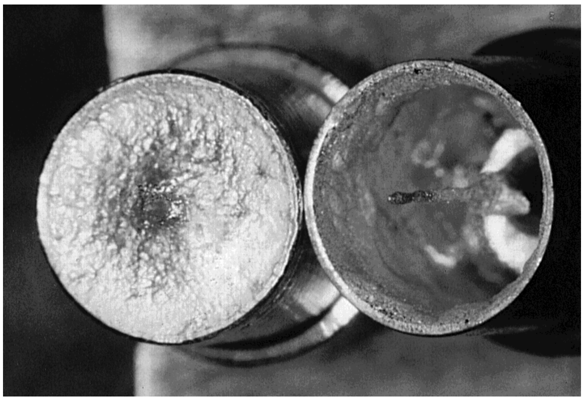

Fig. 1 - LMS1200 reservoir before and after a life-time test

However, this reservoir is still too small for a real application as a thruster. Hence, based on recent mass efficiency results, a new ion emitter has been designed and manufactured with an integrated Indium reservoir of 12 g (see **Fig. 2**) which can operate in a vacuum chamber in any orientation (the capillary forces are predominant) and, hence, in a zero-g environment (free space). This new Indium FEEP ion emitter (V3G model) can provide a total impulse of about 530 Ns at a constant thrust level of 15 µN (assumption: mass efficiency = 50%), that is almost 10000 h of continuous operation at this thrust level.

Fig. 2 – ARCS ion emitters with 0.22, 1.2, and 12 g reservoirs

2.1.2 EXPERIMENTAL SET-UP

ARCS has performed a series of long-term tests using the first prototype of the new V3G ion emitter in the ARCS Large High Vacuum Chamber equipped with an aluminium collector, the QCM diagnostic system, a Probe Scanner for ion beam profile measurements. The V3G1 emitter is mounted on a special CF 150 UHV flange with the necessary low and high voltage UHV feedthroughs, installed centrally on the end flange, which allows to remove the emitter separately from the chamber.
The Indium FEEP emitter can be operated both with a standard HEINZINGER HV power supply (current stabilized mode) and with a thrust stabilizer developed by ARCS wich commands a miniaturized high voltage EMCO module (vacuum compatible); this allows continuous operation at a selected thrust and thrust noise investigation.[7]
The following data are recorded in 2.5 s intervals using BURR-BROWN PCI-20000 series interface cards and KEITHLEY - LABTECH - NOTEBOOK data acquisition software:

- Emitter Voltage
- Emitter Current
- Collector Current
- Chamber Pressure

Furthermore, the accelerator current will be soon included in the data acquisition system (presently, it is manually recorded). Sampling precision of all inputs is 12 bit. The sampled data are stored on the PC's hard disk. Evaluation and presentation of the data is performed using Microcal ORIGIN data analysis and technical graphing software for Windows NT.

2.1.3 15 µN TEST

This test started with a Pre-characterization. **Fig. 3** shows that the thrust has been increased in steps up to 100 µN. For every step an ion beam profile scan has been performed.[6]

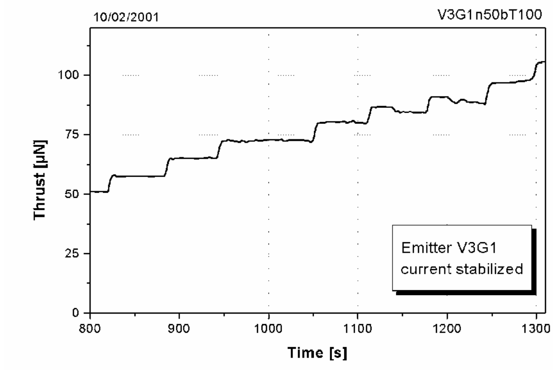

Fig. 3 - Thrust increased in steps up to 100 µN

Fig. 4 shows mass efficiency tests performed with the 12 g V3G1 emitter at different thicknesses of the Indium film covering the emitter needle. The first test was performed immediately after the emitter manufacturing and wetting; the result was a low mass efficiency (5%). After having decreased the Indium film thickness on the needle, the QCM showed a decrease of the Indium film on it (more ion sputtering and less droplet deposition), as shown by the square dots in **Fig. 4.**

This last test was left running for 100 h in order to investigate the long-term behavior of the V3G1 emitter mass efficiency. **Fig. 5** shows that the QCM Indium film decreased with a constant slope (-0.23 nm/h) during the first 2 days of continuous operation at 15 µN. In the third day this decrease slew down; however, the QCM slope was still negative, i.e. ion sputtering was always higher than droplet deposition. Finally, during the fourth day of continuous operation the QCM slope was again about –0.2 nm/h; this means that after 100 h the V3G1 emitter showed the same high mass efficiency as it was at the beginning of the test. Precision weighing of the V3G1 emitter before and after this 100 h test showed that the mean mass efficiency was around 50%.

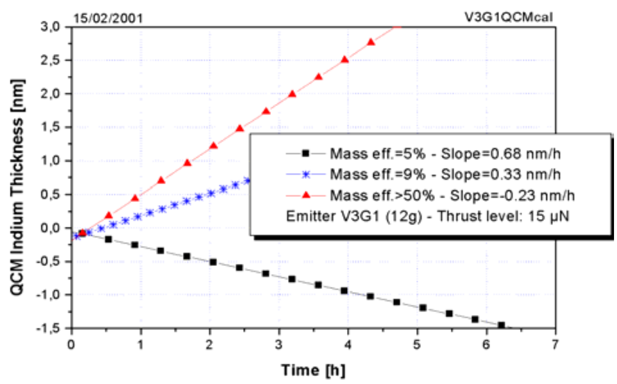

Fig. 4 - Mass efficiency tests performed with the V3G1 emitter at different thicknesses of the needle Indium film

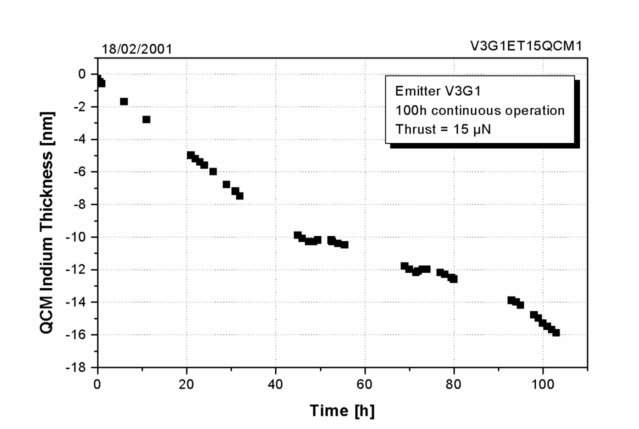

Fig. 5 - QCM reading during the first V3G1 long-term test at 15 µN

The 15 µN test was started in current stabilized mode, i.e. the emitter current was regulated by a standard HEINZINGER HV power supply. In this test the accelerator current was always less than 1 µA, that is less than 1 % of the emitter current.

Fig. 6 shows the thrust calculated from the emitter voltage and collector current. Initially it was unstable, but then it gradually decreased and got more stable, particularly when the V3G1 emitter was operated in thrust stabilized mode during the second day. Unfortunately, the thrust stabilizer had a failure after a day of operation, hence the V3G1 emitter was again operated in current stabilized mode.

Fig. 7 shows the stabilised thrust during the second day of operation; the standard deviation was only 0.72% of the thrust mean value over 24 h of continuous operation.
An Energy Dispersive X-ray (EDX) post-analysis of the apex of this emitter displayed no significant contamination due to stainless steel (coming from the accelerator) or aluminium (coming from the collector) after 100 h of operation at a constant thrust of 15 µN (see **Fig. 8**).

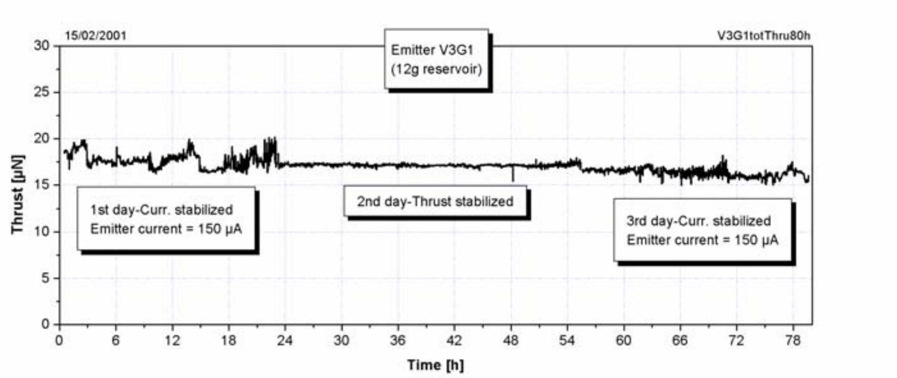

Fig. 6 - Calculated thrust during the first long-term test at 15 µN

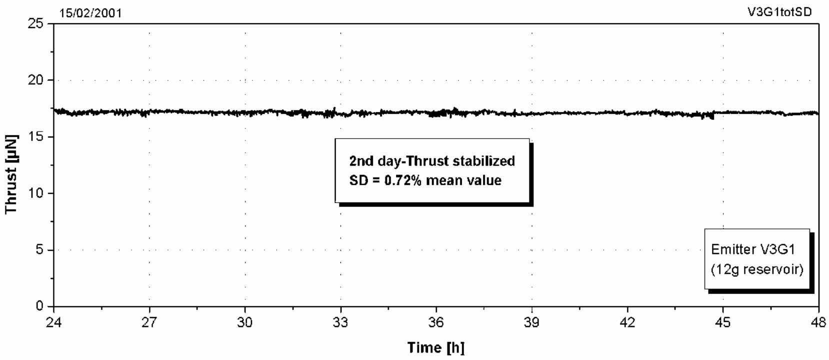

Fig. 7 - Stabilized thrust during the second day of the first V3G1 long-term test at 15 µN

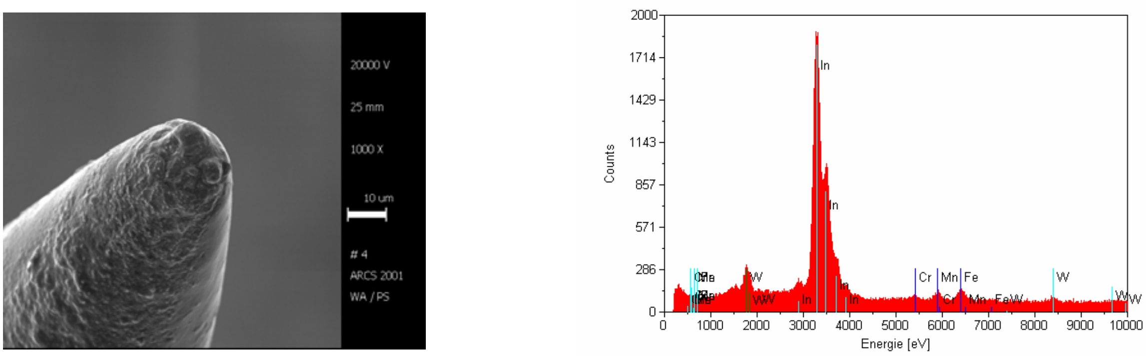

Fig. 8 - EDX analysis of the needle apex of the V3G1 emitter operated at 15 µN in the ARCS Large High Vacuum Chamber (Al collector) for 100 h

2.1.4 75 µN TEST

The noisy operation of the V3G1 emitter in current stabilization mode, as shown in **Fig. 6**, was ascribed to a non-proper wetting of the needle. In fact, after a new wetting, the V3G1 performance at 15 – 20 µN was much more stable, as it can be seen in **Fig. 9** (first 15 hours of operation).

Hence, the thrust level was increased up to around 75 µN. At this high thrust the V3G1 operation in current mode was again noisy, but it got very stable when the V3G1 emitter was operated in thrust stabilized mode. **Fig. 10** shows the stabilised thrust during the second day of operation; the standard deviation was only 0.42% of the thrust mean value over more than 24 h of continuous operation.

The V3G1 mean mass efficiency after 50 h of continuous operation at 75 µN was found to be around 30% precisely weighing the emitter before and after this test. The QCM reading showed a constant sputtering of the crystal, that is a constant instantaneous mass efficiency over more than 24 hours (see **Fig. 11**). Unfortunately, the QCM failure due to excessive sputtering of the crystal prevented further reading.

An EDX post-analysis of the emitter apex displayed no contamination due to stainless steel or aluminium after 50 h of operation at a constant thrust of 75 µN, as shown in **Fig. 12**.

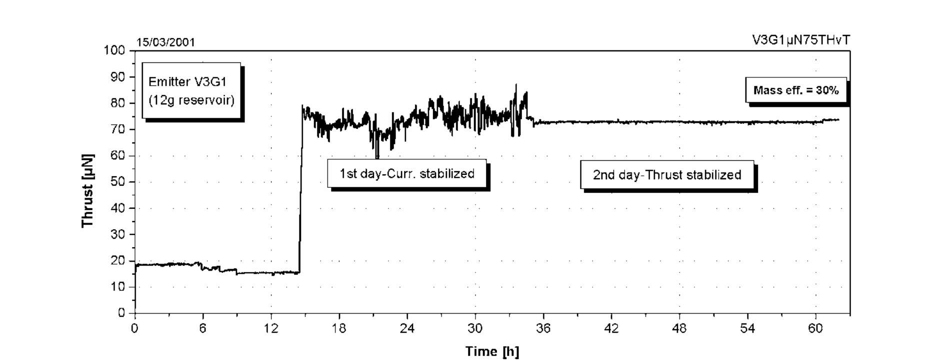

Fig. 9 - Thrust during the V3G1 long-term test at 75 µN

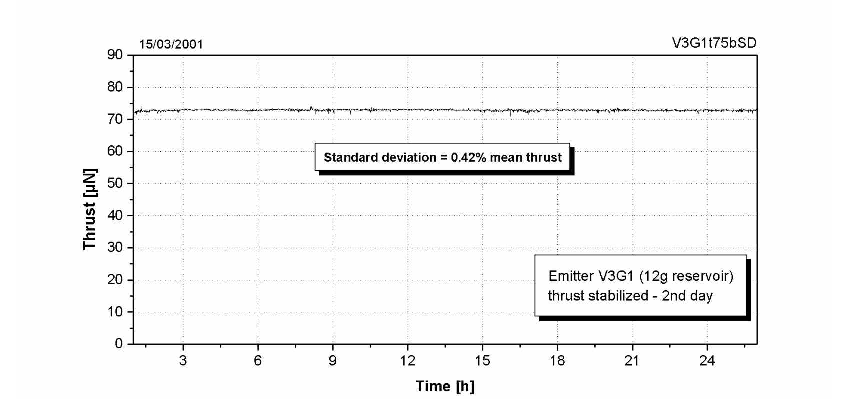

Fig. 10 - Stabilised thrust during the second day of the V3G1 long-term test at 75 µN

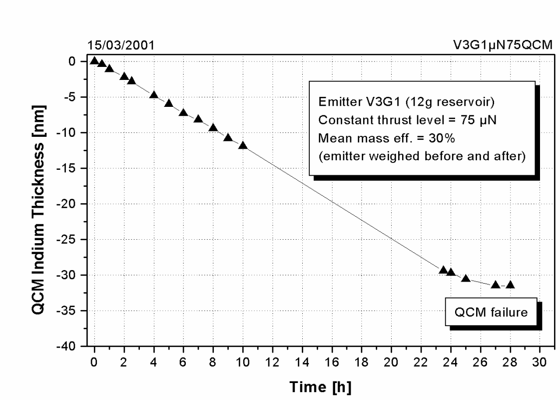

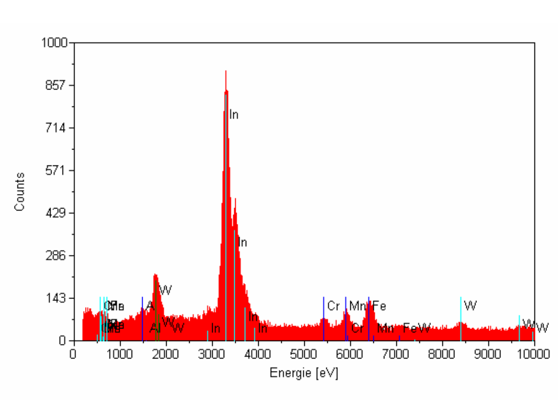

Fig. 11 - QCM reading during the V3G1 long-term test at 75 µN

Fig. 12 - EDX analysis of the needle apex of the V3G1 emitter operated at 75 µN in the ARCS Large High Vacuum Chamber (Al collector) for 50 h

2.1.5 100 µN TEST

The V3G1 emitter was again wetted in order to improve the stability in current mode operation at high thrust levels. After this re-wetting, a new test was started increasing the emitter current (stabilized by a standard HEINZINGER HV power supply) up to 1 mA (see **Fig. 13**), which corresponds to a thrust of around 120 µN. The thruster response is shown in **Figs. 13** (collector current) and **14** (emitter voltage). **Fig. 14** also shows the thrust calculated from the collector current (which corresponds to the ion beam current) and the emitter voltage. These graphs highlight that The V3G1 operation in current stabilization mode was very stable up to a thrust level of 75 µN; the difference between the emitter current and the collector current (which corresponds to the accelerator current) was practically zero up to this thrust level, and the emitter voltage was also quite stable.

This test went on keeping the emitter current at 800 µA (~ 100 µN) for several hours. **Fig. 15** shows that even in current stabilization mode (open loop) the standard deviation was only 2.1% of a mean thrust value of 99.7 µN over more than 4 hours of continuous operation.

After a new re-wetting of the emitter needle, the thruster displayed a very stable operation in current mode even at a thrust level of 100 µN, as it can be seen in **Fig. 16**.

In order to assess the Indium FEEP Microthruster capability to perform a certain thrust profile, the emitter voltage was commanded using a sinusoidal profile between 3 kV (below the emitter threshold voltage) and 9.5 kV. **Fig. 17** shows the thruster response in terms of calculated thrust, which ranged from 0 to 85 µN with a high reproducibility.

At present, the first prototype of the new V3G ion emitter has accumulated more than 700 hours of cumulative operation using the original Indium charge (12 g). This is a good indication of the effectiveness of the new large integrated Indium reservoir.

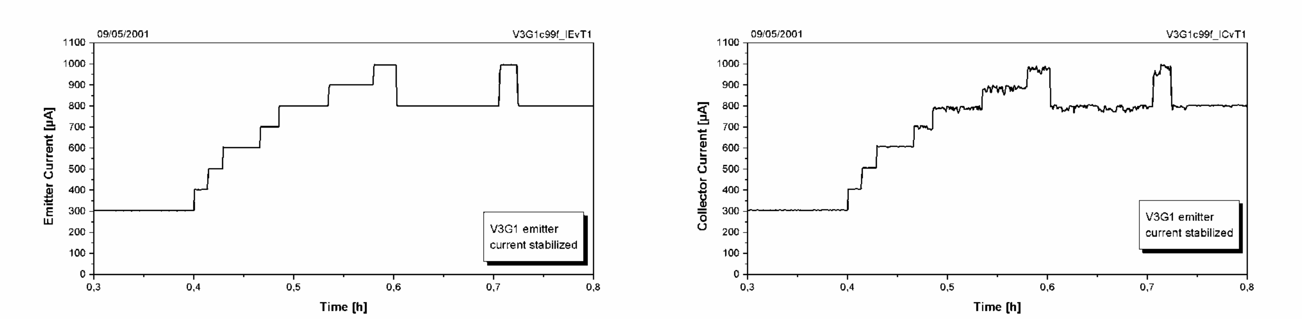

Fig. 13 - Emitter and collector currents during the burn-in phase of a V3G1 test at 100 µN

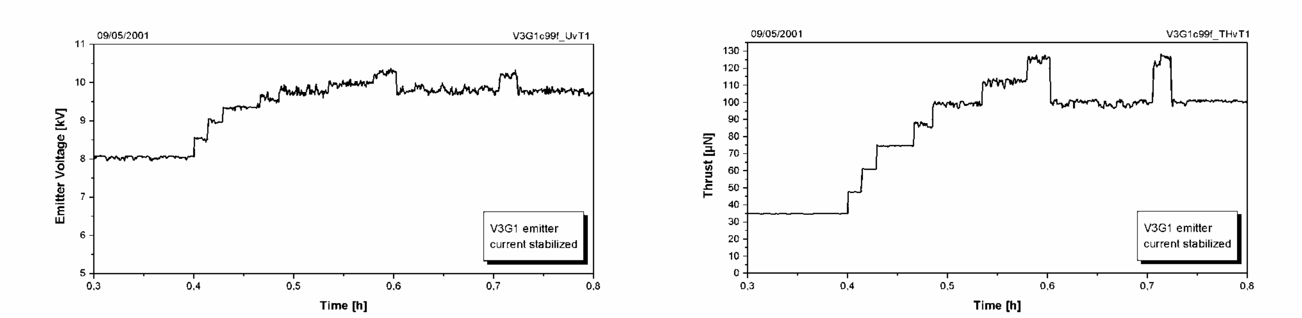

Fig. 14 - Emitter voltage and calculated thrust during the burn-in phase of a V3G1 test at 100 µN

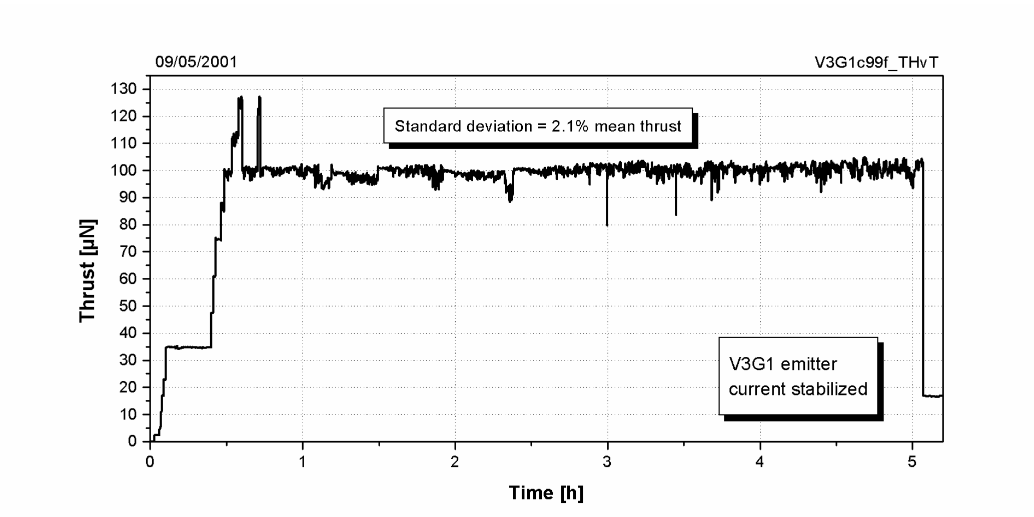

Fig. 15 - Calculated Thrust during a 4.5 h V3G1 test at 100 µN

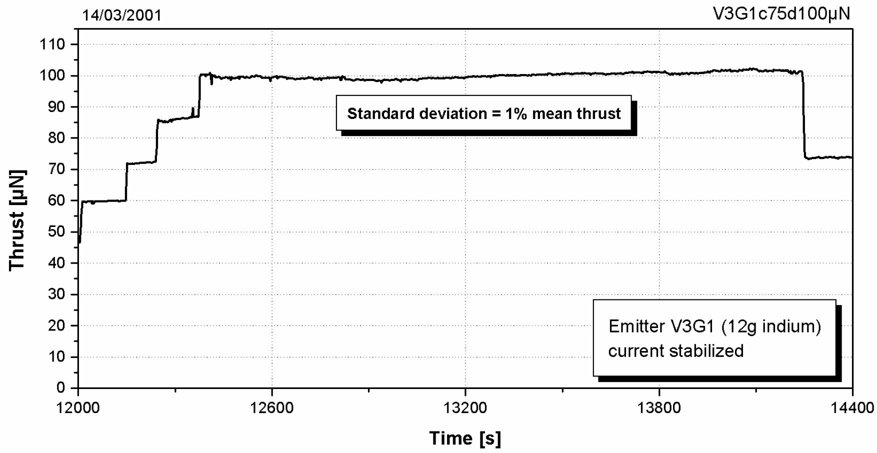

Fig. 16 - 100 µN step of 2000 s in current stabilization mode (open loop)

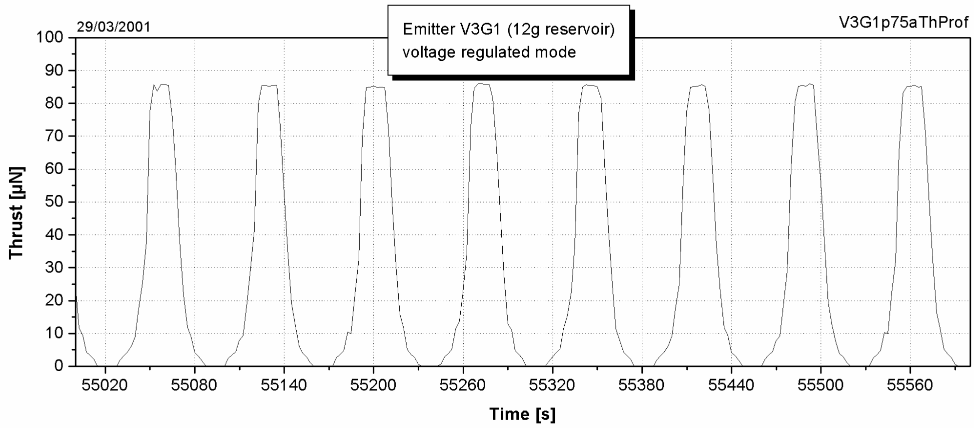

Fig. 17 - Thruster response in terms of calculated thrust

2.2 Endurance Testing

2.2.1 Experimental Set-up

Two vacuum facilities are available at ARC for endurance testing. The first one, the Large Indium FEEP Test Facility # 1 (LIFET 1), consists of a cylindrical, stainless steel vessel of around 1.0 m of diameter, 1.5 m of length and a volume of 1.2 m^3. The pumping system of the LIFET 1 consists of:

- fore-pump, Pfeiffer Balzers DUO 030 A (30 m^3/h)
- turbo-pump, Pfeiffer Balzers TPU 2200 (2200 l/s)

An automatic pumping unit controls both the fore-pump and the turbo-pump. To enhance the final vacuum, the vacuum chamber can be outgassed at about 100° C. Presently, the vacuum level obtained is in the order of 10^{-7} mbar. The pressure in the chamber is measured with a PENNING gauge (BALZERS IKR 010) and a hot-cathode Bayard-Alpert gauge (BALZERS IM 15). An aluminium ion beam collector has been mounted inside the chamber. It has a chevron configuration, which results in large angles (typically greater than 50 degrees) between the expected ion trajectories and the direction normal to the aluminium surface. This allows to reduce both the collector sputtering yield and the amount of sputtered material directed back towards the thruster. The current density distribution in the ion beam can be measured by electrostatic wire probes[7]. The Indium FEEP Microthruster is mounted on a special CF 150 UHV flange with the necessary low and high voltage UHV feedthroughs, installed centrally on the end flange, which allows to remove the emitter separately from the chamber (see **Fig. 18**).

The following data are recorded in 2.5 s intervals using BURR-BROWN PCI-20000 series interface cards and KEITHLEY - LABTECH - NOTEBOOK data acquisition software:

- Emitter Voltage
- Emitter Current
- Collector Current
- Chamber Pressure

Furthermore, the accelerator current is measured by an analogue amperemeter.
Sampling precision of all inputs is 12 bit. The sampled data are stored on the PC's hard disk. Evaluation and presentation of the data is performed using Microcal ORIGIN data analysis and technical graphing software for Windows NT.

The second Large Indium FEEP Test Facility, LIFET 2, includes a cylindrical, stainless steel vacuum chamber of around 0.8 m of diameter, 1.8 m of length and a volume of 0.9 m^3. The pumping system of the LIFET 2 consists of:

- fore-pump, Balzers DUO 35 (35 m^3/h)
- turbo-pump, Pfeiffer TPU 510 (500 l/s)

Presently, the vacuum level obtained is in the order of 10^{-6} mbar. The pressure in the chamber is measured with a PENNING gauge (BALZERS IKR 010). An aluminium ion beam collector has been mounted inside the chamber. It has a closed configuration in order to completely shield the chamber walls; as mentioned before, this allows measurements of the actual ion beam current. The Data Acquisition System consists of a KEITHLEY Data Acquisition Card and TESTPOINT software.

Fig. 18 - Left image: ARC Large High Vacuum Chamber No. 1; right image: aluminum collector inside the vacuum chamber

2.2.2 17 µN Endurance Test

The microthruster tested (V3L7 model) was of the needle type with a reservoir containing 1.2 g of Indium. **Fig. 19** shows the ion emitter which includes the Indium reservoir and the tungsten needle. This Indium FEEP Microthruster was mounted in the LIFET 1. This endurance test started on the 21st of July, 2001, setting the emitter current (stabilised by a standard HEINZINGER HV power supply) to a constant value of about 150 µA (see **Fig. 20**), which corresponds to a thrust of about 17 µN. This thrust level is consistent with the requirements of several new scientific missions, such as SMART 2, LISA, DARWIN and TPF.

Fig. 21 shows a comparison between the emitter current and the collector current, which is the actual ion beam current. The difference between these two currents, which represents the extractor current, was practically negligible over the whole test, as it can be seen in **Fig. 22** which shows that the collector current stayed very stable over more than 800 hours of continuous operation. In fact, the test ended on the 24th of August, 2001, with the total consumption of the propellant. This is a good indication of the effectiveness of the integrated Indium zero-g reservoir, which uses capillary forces in order to supply the needle with the liquid metal.

Fig. 23 shows the emitter voltage during the 17 µN Endurance Test. Post-test visual inspection found out no indication of electrode erosion and needle de-wetting (end of life - due to lack of In), but only a small decrease of the extractor hole due to Indium droplet deposition. This caused the 1 kV decrease in the emitter voltage after around 500 h of continuous operation. This is in line with the results of the lifetime prediction model, estimating a slow closing of the extractor due to microdroplet deposition.

Fig. 24 shows the calculated thrust during the 17 μN Endurance Test. The results show a good thrust stability even in current stabilised mode (open loop). In fact, the standard deviation is only 3.5% of the mean value (17.1 μN); however, in thrust stabilisation mode (closed loop) the standard deviation can be 10 times lower[5-6].

Mass efficiency is an important parameter describing the amount of propellant emitted in the form of unionised neutral microdroplets which do not contribute to thrust. In order to estimate this parameter on-line during thruster operation, a Quartz Crystal Microbalance (QCM) was installed in the LIFET 1, at the base of the collector aligned to the ion emitter. With proper calibration by standard mass loss measurement, the QCM can give real-time mass efficiency reading during long term test runs of Indium FEEP thrusters.

In a mixed ion/droplet beam, as for every Liquid Metal Ion Source including FEEP thrusters, both material deposition and material erosion (sputtering) are taking place simultaneously on the QCM. The droplet component is responsible for the deposition (sputtering effect negligible) and the ion component is responsible for the sputtering, both from the original substrate and the droplets deposited by the beam itself.

Fig. 25 shows that the QCM reading decreased with a constant slope (-2.5 nm/day) during the first 6 days of continuous operation at 17 μN, i.e. ion sputtering was higher than droplet deposition. Then, the slope changed to about –1.3 nm/day, and it stayed constant for the rest of the test. This means that the instantaneous mass efficiency was constant over more than 800 hours of continuous operation, except for a small change after 6 days. Using the proper calibration for the QCM, we obtain mass efficiency values of 63% and 42% for the first and second part of the test run respectively.

Precision weighing of the microthruster before and after this endurance test showed that the mean mass efficiency was 45%. A short test performed with the same microthruster using the last milligrams of Indium left in the reservoir showed the same value for the mass efficiency.

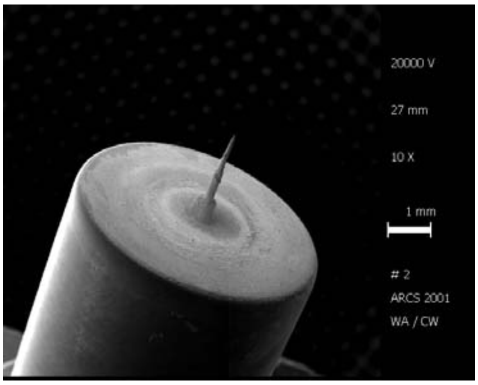

Fig. 19 - V3L7 Indium FEEP ion emitter.

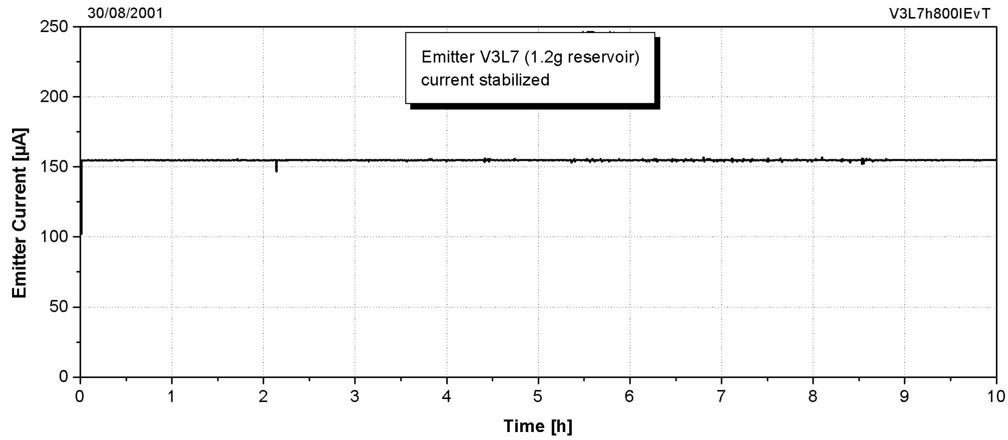

Fig. 20 – Emitter current versus time

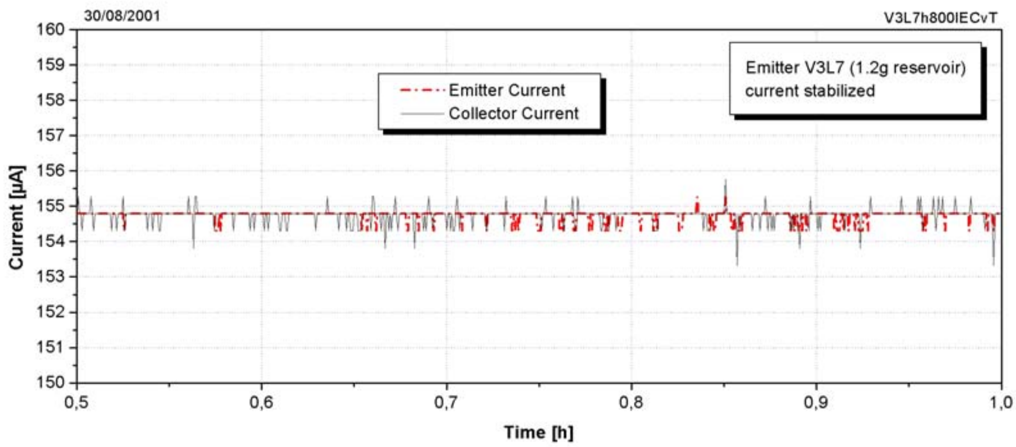

Fig. 21 – Comparison between emitter current and collector current (small scale, 1 Bit resolution).

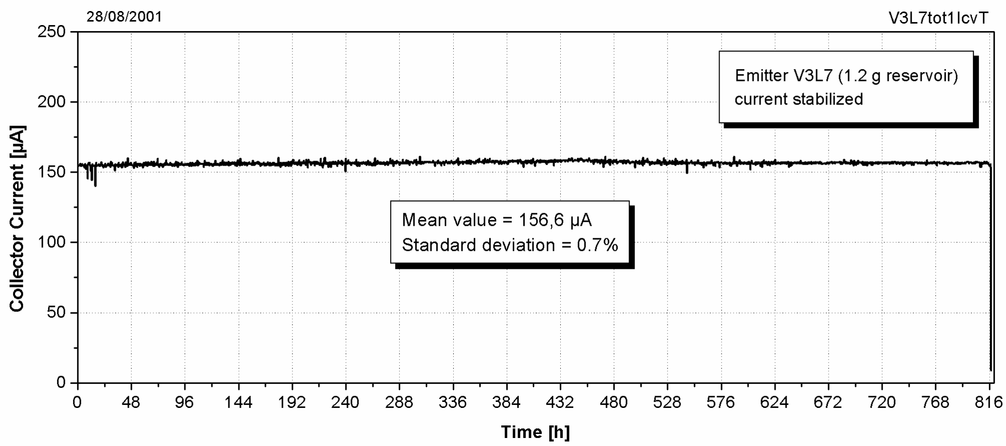

Fig. 22 – Collector current during the 17 µN Endurance Test

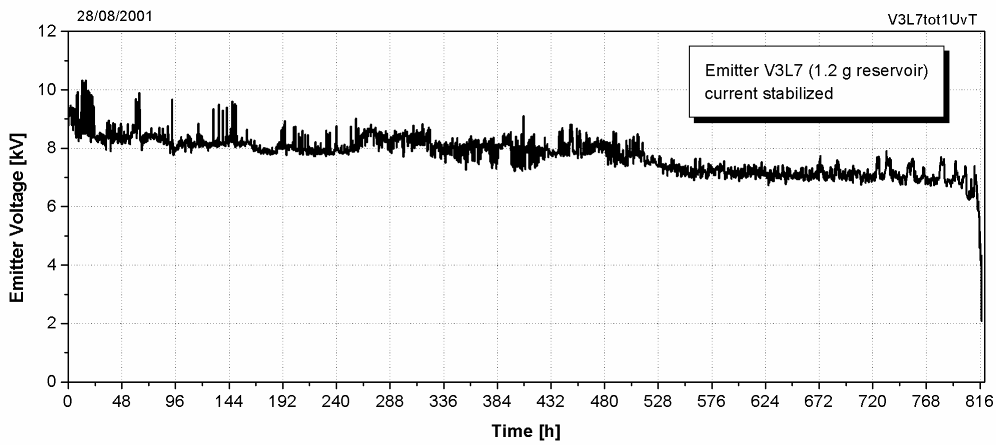

Fig. 23 – Emitter voltage during the 17 µN Endurance Test.

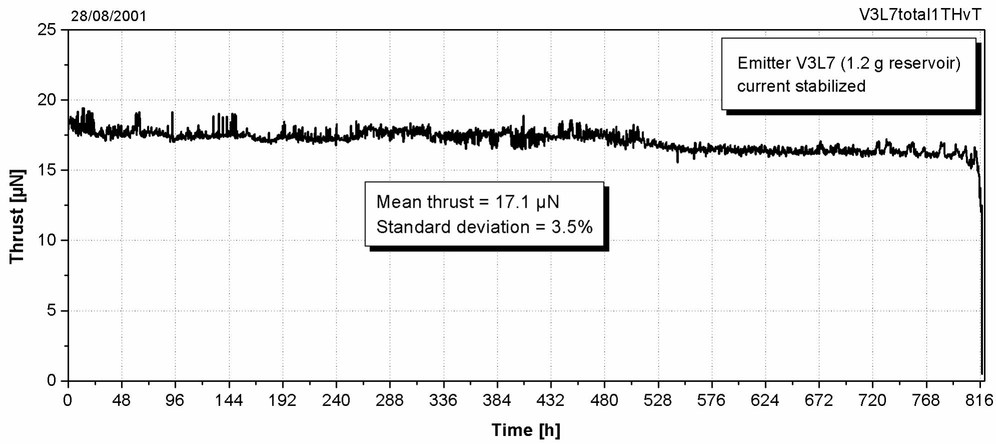

Fig. 24 – Calculated thrust during the 17 µN Endurance Test.

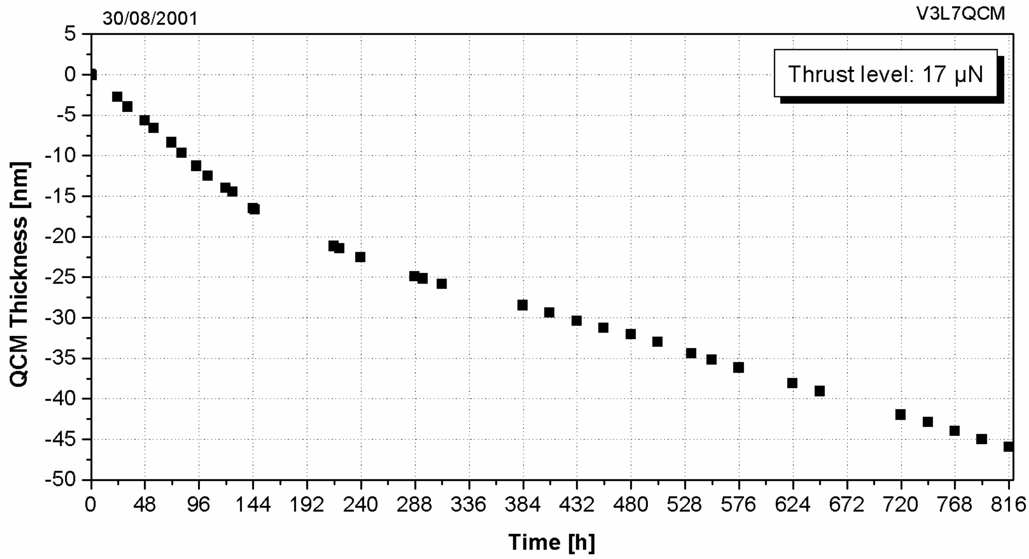

Fig. 25 – QCM reading during the 17 µN Endurance Test.

2.2.3 0-35 µN Endurance Test

The second endurance test was started in the LIFET 1 on the 25th of August, 2001. The microthruster tested (V3R1 model) was of the needle type with a reservoir containing 1.2 g of Indium.

This test was performed commanding a sin^6 profile for the emitter current from 0 to 350 µA, with a period of 5000 s, as shown in **Fig. 26** (nominal operation). This leads to a thrust profile from 0 to about 35 µN. Furthermore, once per week a half-sinus profile with 0.1 Hz frequency and 250 µA amplitude was superimposed to the nominal profile for 6 hours (calibration phase). The total thrust peak of both is then about 60 µN. This was done according to the requirements of the GOCE mission.

Fig. 27 shows the thruster response in terms of emitter voltage. The two threshold voltages (ion emission on and off) are clearly visible. It is interesting to note that for this emitter the on-voltage (~4.6 kV) was higher than the off-voltage (~3.4 kV). Then, the emitter voltage followed the current according to the thruster characteristic; it ranged from 4.6 kV (1 µA) to about 6 kV (350 µA) and then down to 3.4 kV.

Fig. 28 shows the collector current, which is the actual ion beam current. **Fig. 29** shows a comparison between the emitter current and the collector current. The difference between these two currents, which represents the extractor current, was less than 10 µA at the maximum emitter current (350 µA), and it stayed below 5% of the emitter current over the whole endurance test.

Fig. 30 shows the thrust calculated from the emitter voltage shown in **Fig. 27** and the collector current in **Fig. 28**. The thrust ranges from 0 to about 35 µN with a good reproducibility. **Fig. 31** is an enlargement of the previous graph; it shows that very low thrust levels can be commanded, even below 0.1 µN.

Fig. 32 shows the start of the first calibration phase, that is once per week a half-sinus profile with 0.1 Hz frequency and 250 µA amplitude superimposed to the nominal profile for 6 hours. The total thrust peak of both is then about 60 µN, as shown in the enlargement in **Fig. 33**. A total of 6500 calibration cycles have been performed during this test (three calibration phases each of 6 hours).

Fig. 34 shows the emitter voltage during the 0-35 µN Endurance Test. The peak voltage corresponding to 350 µA fluctuated between 6 and 7 kV during the test.
Fig. 35 shows the collector current; the three calibration phases, each of 6 hours, are clearly observable.

Fig. 36 shows the calculated thrust over about 460 hours of continuous operation with the emitter current ranging from 0 to 350 µA. This means 330 on-off cycles without any significant performance degradation. The fluctuation of the peak thrust observable in **Fig. 36** is not real, but is due to a failure of the Microcal ORIGIN data analysis and technical graphing software in plotting so many data. In fact, this is not observable in the enlargement in **Fig. 37**. Here, the peak thrust stayed quite constant to a value of 35 µN and it increased up to 60 µN during the three calibration phases. However, in this test only the emitter current is controlled; hence, the thrust follows the behaviour of the emitter voltage. This can be easily settled by controlling both the current and the voltage in a closed loop.

Precision weighing of the microthruster before and after this endurance test showed that the mean mass efficiency was 18%. This low value is due to the fact that it was not possible (due to time constraints) to start this test with an emitter being specially treated for high mass efficiency.

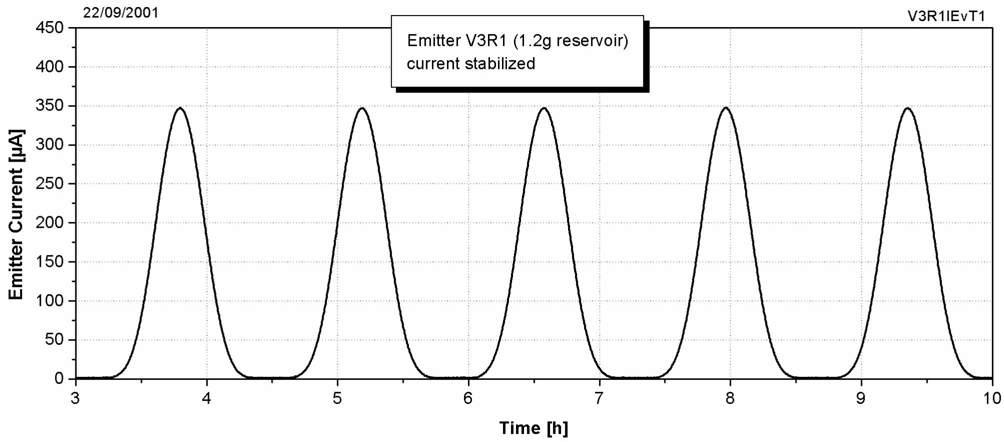

Fig. 26 – Emitter current versus time

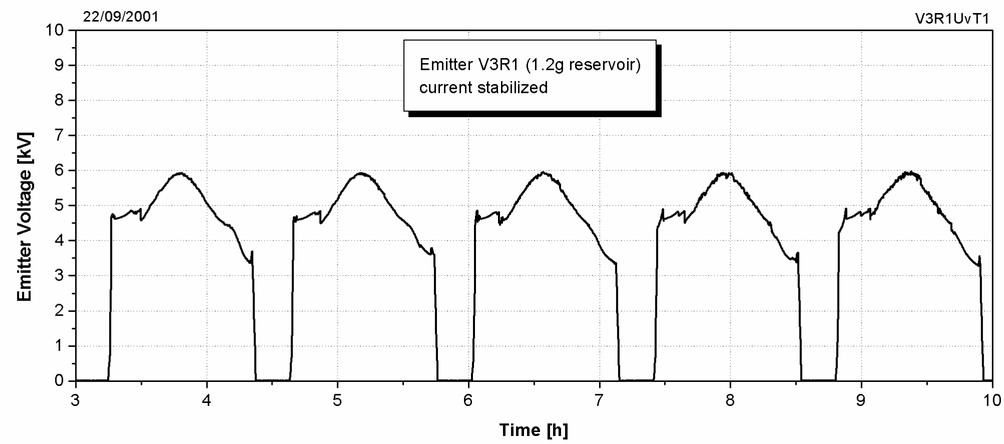

Fig. 27 – Emitter voltage versus time

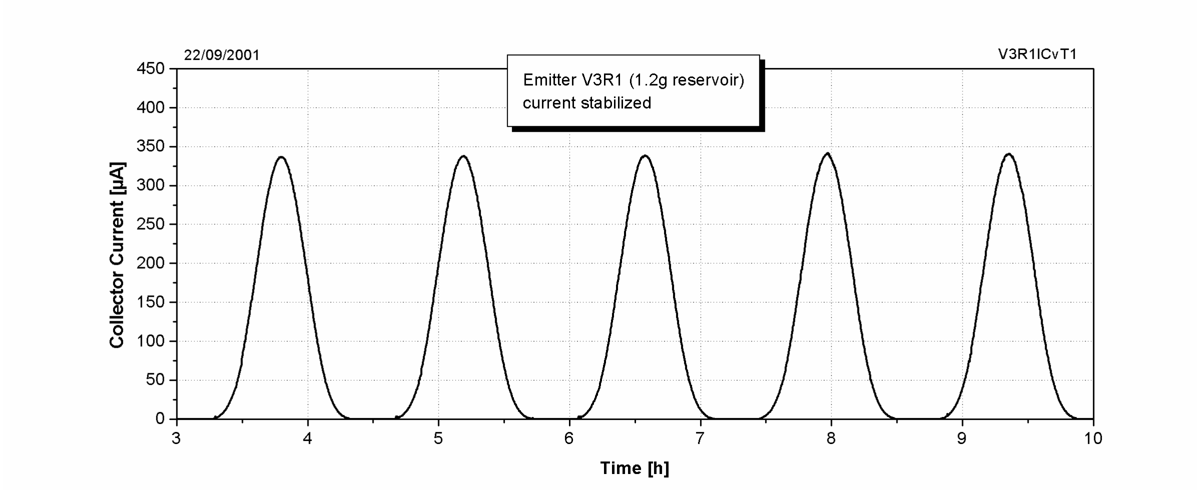

Fig. 28 – Collector current versus time

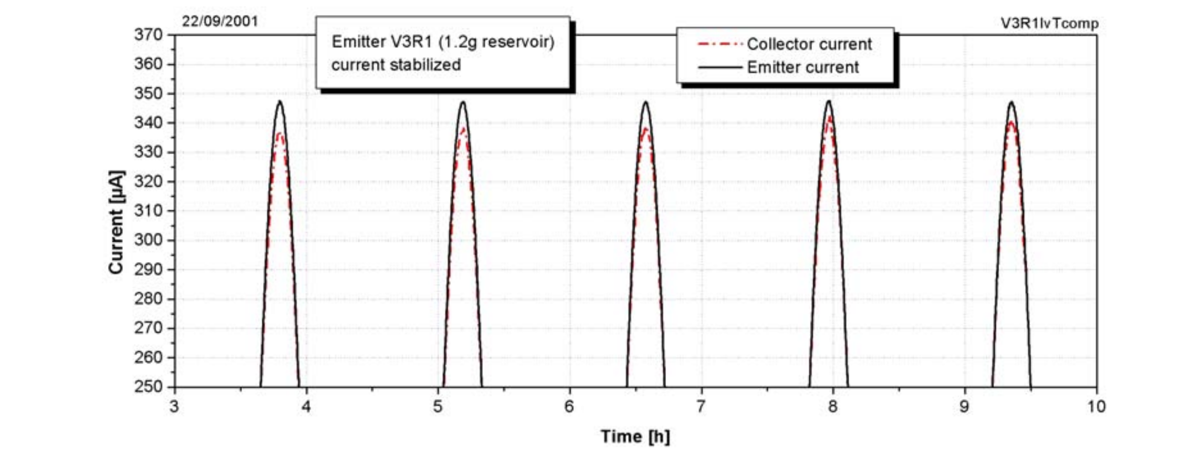

Fig. 29 – Comparison between emitter current and collector current

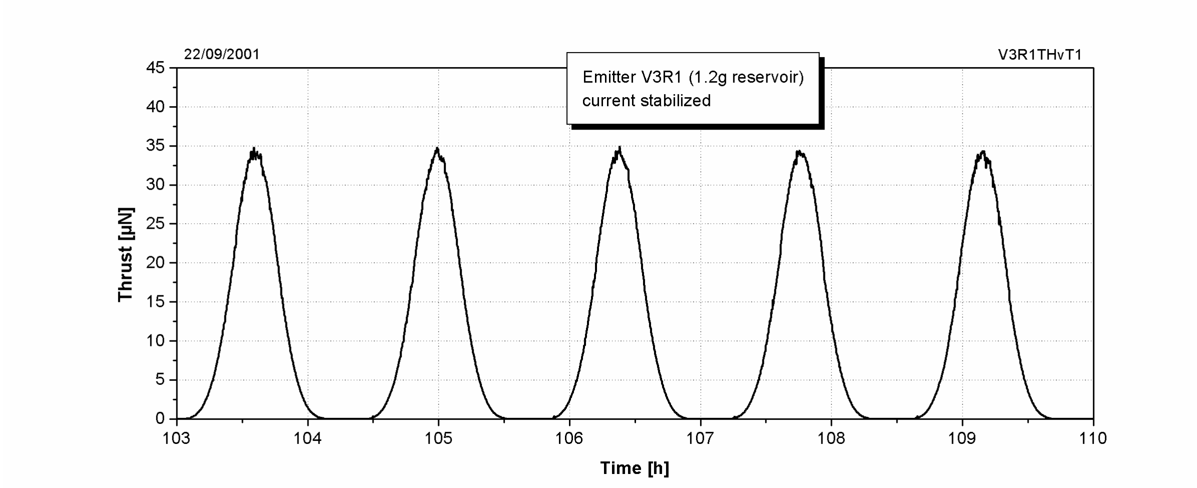

Fig. 30 – Calculated thrust versus time

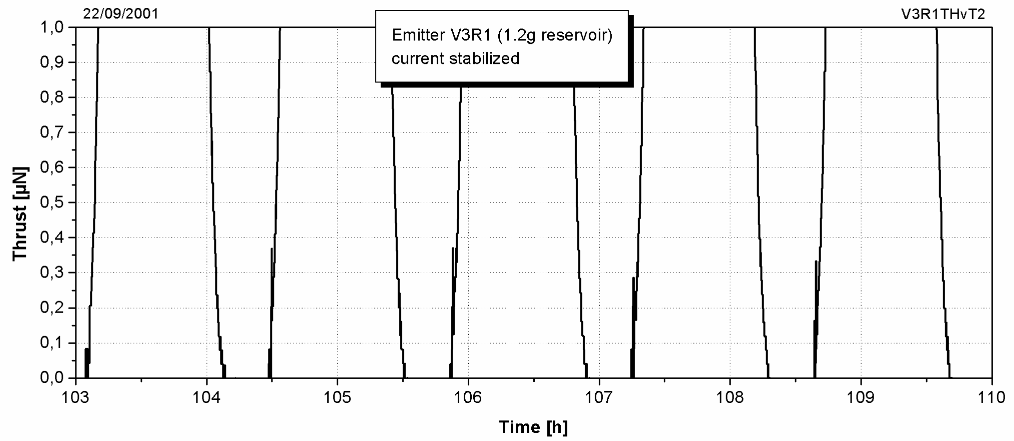

Fig. 31 – Calculated thrust versus time; enlargement.

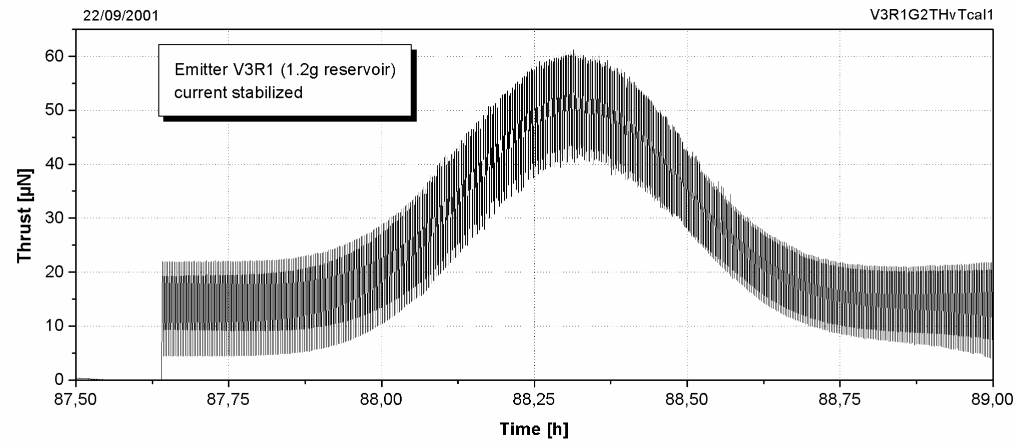

Fig. 32 – Calculated thrust versus time during the calibration phase.

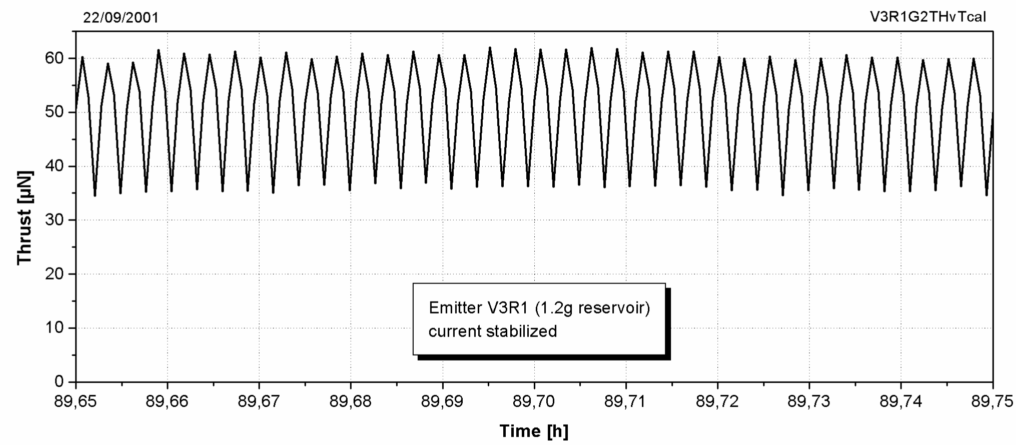

Fig. 33 – Calculated thrust versus time during the calibration phase; enlargement.

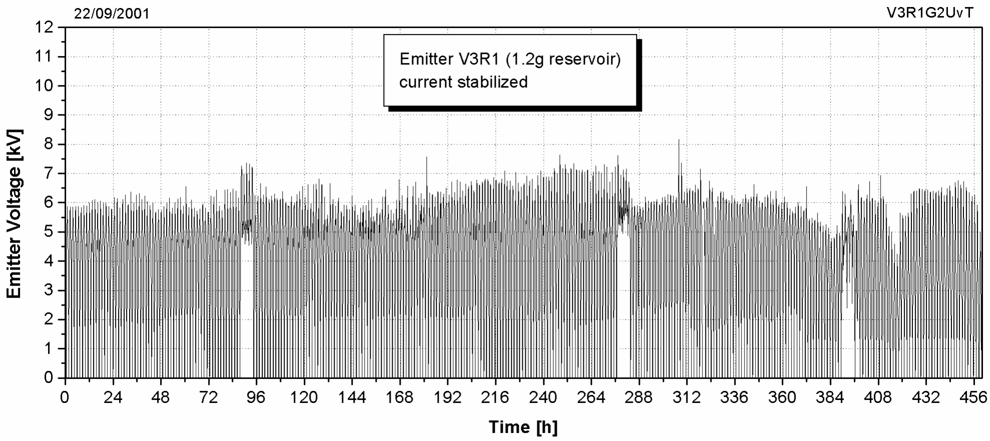

Fig. 34 – Emitter voltage during the 0-35 µN Endurance Test.

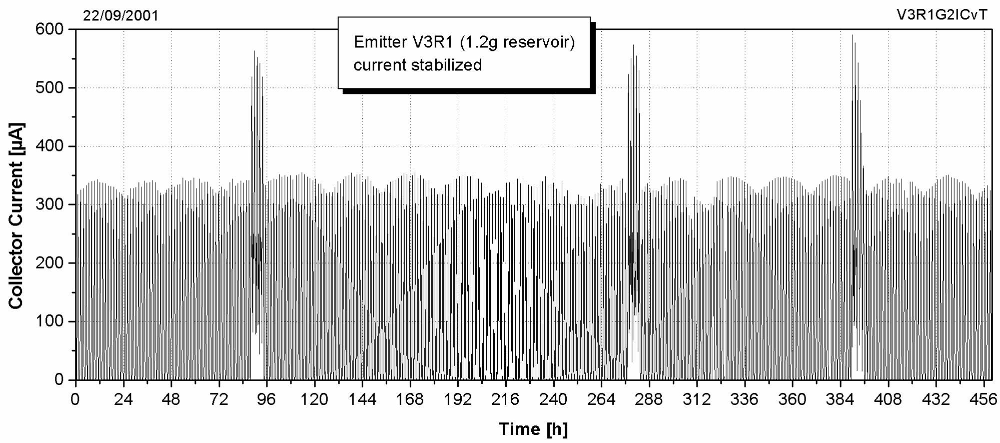

Fig. 35 – Collector current during the 0-35 µN Endurance Test.

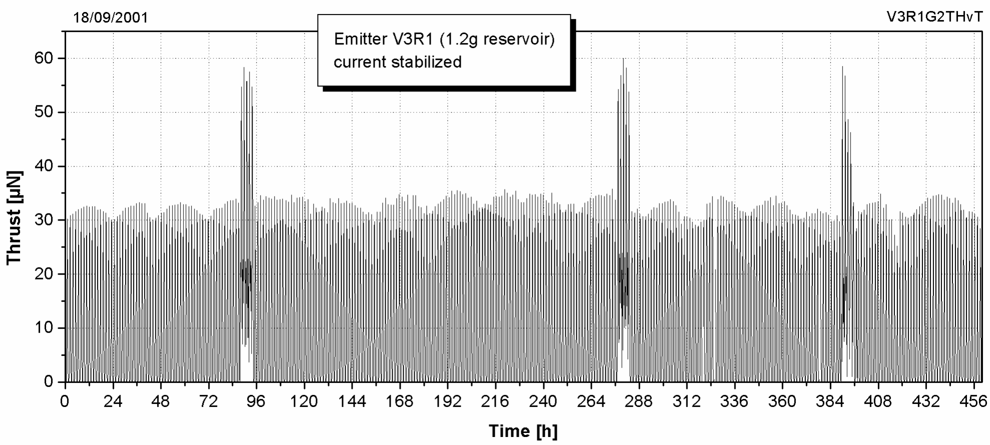

Fig. 36 – Calculated thrust during the 0-35 µN Endurance Test.

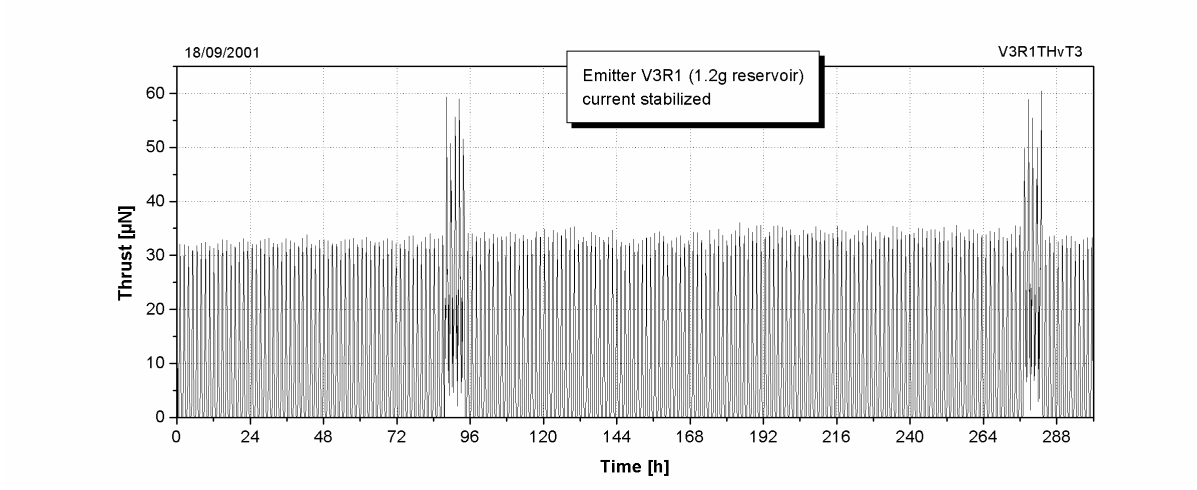

Fig. 37 – Calculated thrust during the 0-35 µN Endurance Test; enlargement.

2.2.4 0-25 µN Endurance Test

The third endurance test was started in the LIFET 2 on the 20th of August, 2001. The microthruster tested (V3LOR2 model) was of the needle type with a reservoir containing 1.2 g of Indium.

This test was performed commanding a half-sinus profile for the emitter current from 0 to 250 µA, with a period of 5000 s. This leads to a thrust profile from 0 to about 25 µN, as shown in **Fig. 38**. **Fig. 39** shows the thruster response in terms of emitter voltage. The two threshold voltages (ion emission on and off) are clearly visible, and they have almost the same value for this emitter.

Fig. 40 shows the calculated thrust over about 470 hours of continuous operation with the emitter current ranging from 0 to 250 µA. This means 340 on-off cycles without any significant performance degradation. The peak thrust is not constant because in this test only the emitter current is controlled; hence, the thrust follows the behaviour of the emitter voltage. This can be easily settled by controlling both the current and the voltage in a closed loop. The sudden decrease of the thrust after 470 h of operation corresponds to the total consumption of the propellant.

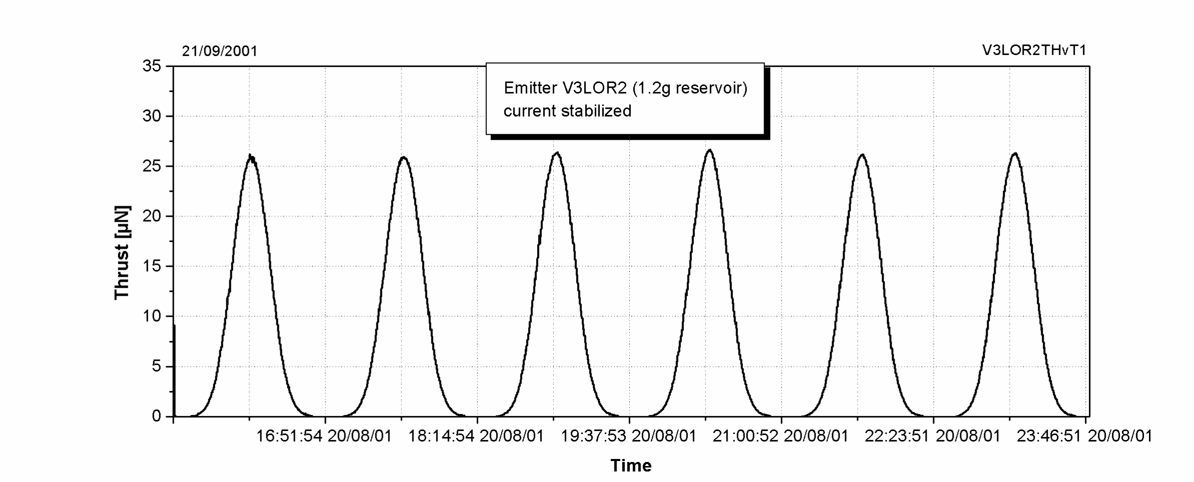

Fig. 38 – Calculated thrust versus time (0-25 µN Endurance Test).

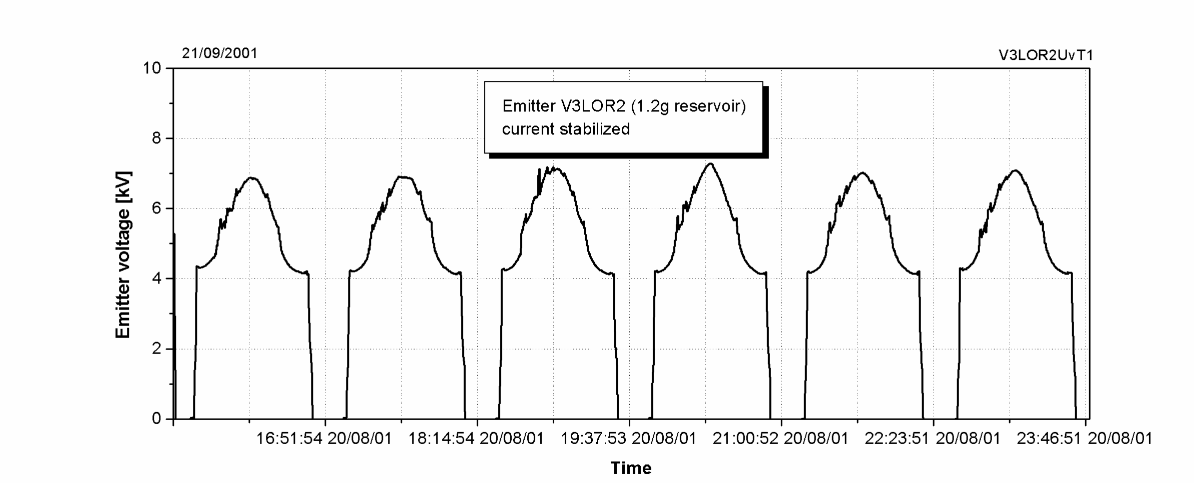

Fig. 39 – Emitter voltage versus time (0-25 µN Endurance Test).

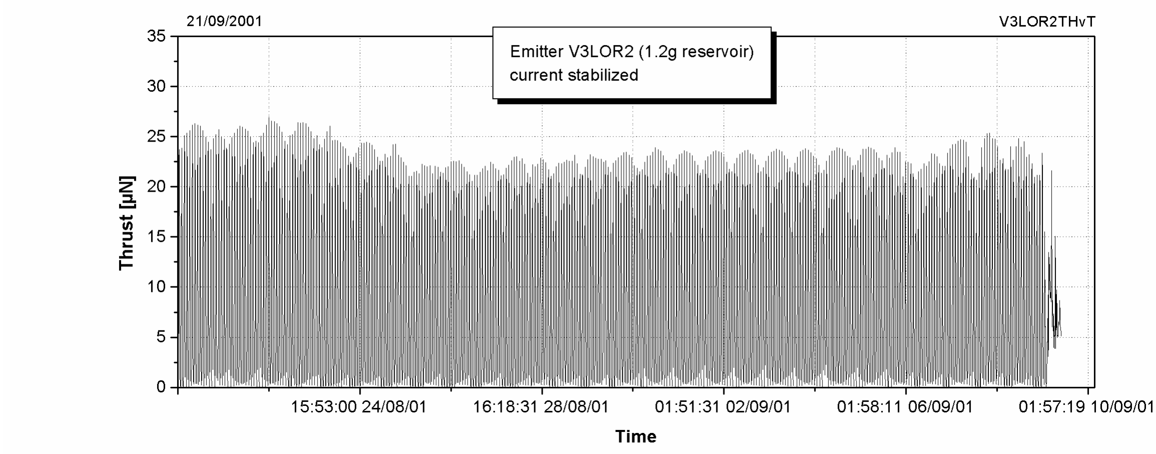

Fig. 40 – Calculated thrust during the 0-25 µN Endurance Test .

3 ANNEX B – CLUSTER TESTING

3.1 Introduction

The Indium FEEP propulsion system has recently gained considerable attention for several new scientific applications which need drag-free attitude control and ultraprecise pointing. This is the case for the Gravity field and steady state Ocean Circulation Explorer (GOCE) which aims to provide global and regional models of the Earth's gravity field and of the geoid, its reference equipotential surface, with high spatial resolution and accuracy experiments (thrust level up to 1.2 mN). In view of this short-term application opportunity, it is mandatory to demonstrate the proper operation of a cluster of Indium FEEP Microthrusters. In fact, the thruster to be tested is based on the space-proven ARCS indium ion emitter and can provide a continuous thrust between 1 to 75 µN. This microthruster can also operate at a peak thrust of 100 µN for short periods. Hence, by clustering this "building block" it is possible to reach higher thrust levels.

3.2 Cluster Test Definition

The indium FEEP microthruster selected for this cluster test will be the new In-FEEP 100 model. It is based on the space-proven ARCS indium ion emitter (see Figs. 1 and 2) which can provide a continuous thrust between 1 to 75 µN with an accuracy of 0.1 µN and a very low thrust noise (< 0.1 µN over periods of more than 1000 s), and a peak thrust of 100 µN (see Fig. 3). Hence, 12 of these emitters can fulfil the GOCE thrust requirements (1 µN – 1mN), that is up to 650 µN continuously and a maximum thrust of up to 1.2 mN for short periods. In fact, GOCE needs the highest thrust level (1.2 mN) only for the instrument calibration, whereas the measurement phase needs a lower thrust level.

The ARCS indium ion emitter is integrated in a module, which provides the necessary housing, thermal insulation and electrical connections. This module is built around the emitter and can be used like a plug-in device having standard mechanical and electrical interfaces. Fig. 4 shows an Indium FEEP module.

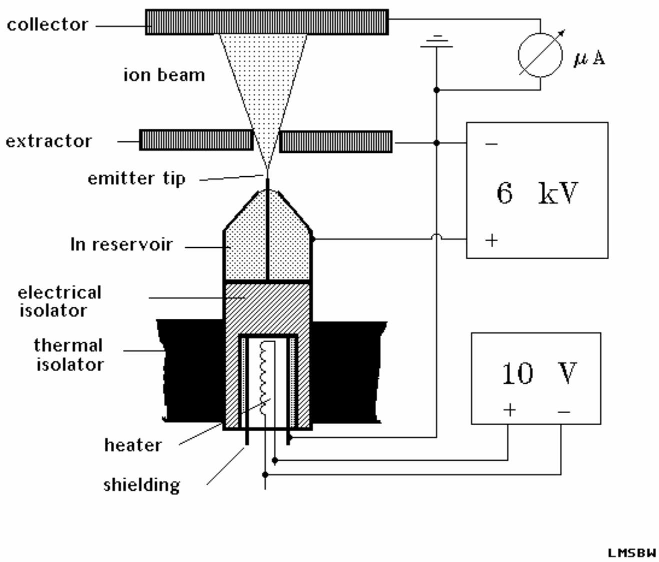

Fig. 1 – Schematic drawing of the operating principle of the ARCS indium ion emitter

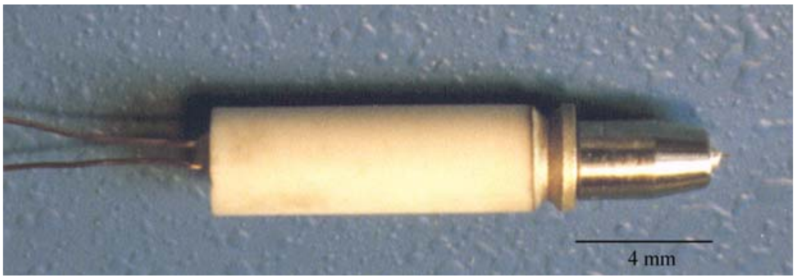

Fig. 2 – Indium ion emitter developed at Seibersdorf (length: 19 mm; diameter: 4 mm; weight: 1.2 g)

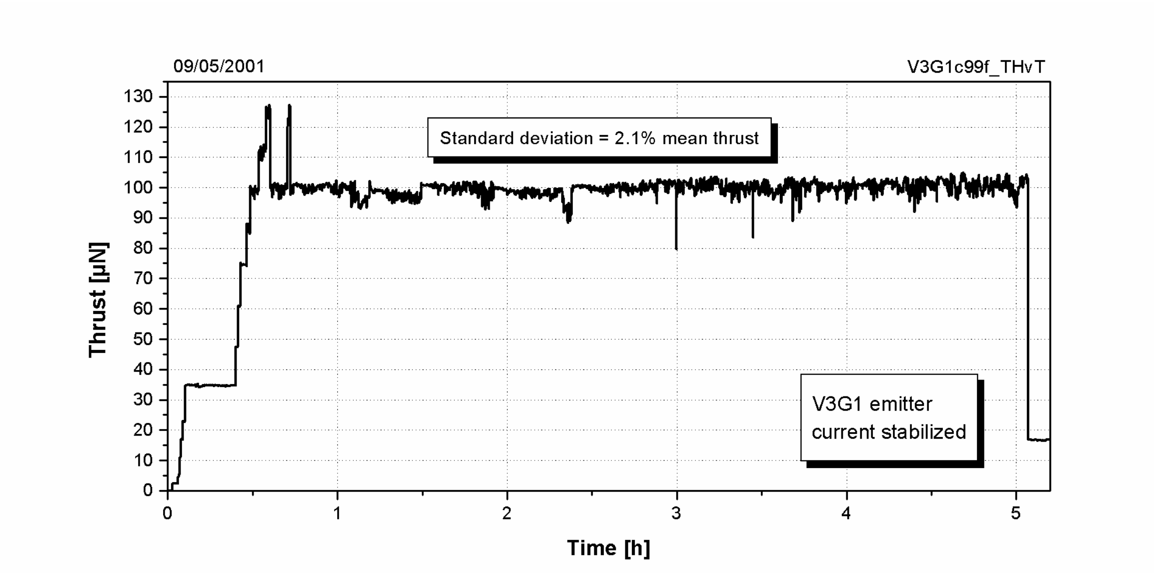

Fig. 3 Calculated Thrust during a 4.5 h test at 100 µN

Fig. 4 – Indium FEEP Module (diameter: 44 mm; height: 52 mm; weight: 95 g)

Three of these modules will be tested in a cluster configuration firing in the same direction (maximum thrust of 300 µN). This is considered a good compromise in order to investigate the behaviour of Indium FEEP Microthrusters firing simultaneously at close distance (interaction between the ion beams, high voltage insulation, overall thrust noise...). In fact, a cluster of 12 modules would need many more time and financial resources than the ones foreseen for this pre-qualification phase. However, this test will be the first one on a cluster of FEEP (either cesium or indium) microthrusters, hence the results gathered will be very important for all scientific missions which need a multi-thruster assembly for high thrust levels and/or high redundancy. The three modules will be clustered in order to have the three indium emitters at the vertices of an equilateral triangle (see Fig. 5).

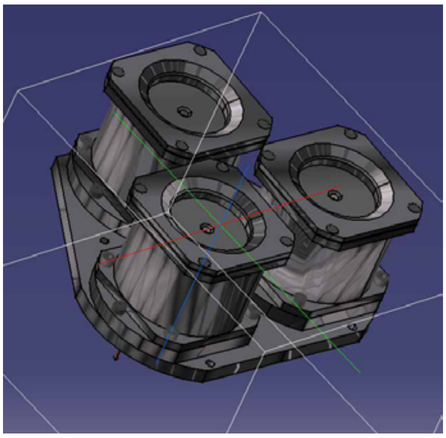

Fig. 5 – Artist´s concept of the Indium FEEP Cluster

3.3 Experimental Set-up

Vacuum Facility

The cluster test will be performed in a large high vacuum chamber located in the ARCS indium FEEP laboratory (see Fig. 6).

Fig. 6 – Indium FEEP laboratory: ARCS Large High Vacuum Chamber (dia. = 1 m, length = 1.5 m, volume = 1.2 m^3)

This facility consists of a cylindrical, stainless steel vessel of around 1.0 m of diameter, 1.5 m of length and a volume of 1.2 m^3. The pumping system of the ARCS FEEP Large High Vacuum Chamber consists of:

- fore-pump, Pfeiffer Balzers DUO 030 A (30 m^3/h)
- turbo-pump, Pfeiffer Balzers TPU 2200 (2200 l/s)

An automatic pumping unit controls both the fore-pump and the turbo-pump. To enhance the final vacuum, the vacuum chamber can be outgassed at about 100° C. Presently, the vacuum level obtained is in the order of 10^{-7} mbar. The pressure in the chamber is measured with a PENNING gauge (BALZERS IKR 010) and a hot-cathode Bayard-Alpert gauge (BALZERS IM 15).

An aluminium ion beam collector will be mounted inside the chamber. It will have a chevron configuration, which results in large angles (typically greater than 50 degrees) between the expected ion trajectories and the direction normal to the aluminium surface. This allows to reduce both the collector sputtering yield and the amount of sputtered material directed back towards the thruster.

The current density distribution in the ion beam will be measured by electrostatic probes, which will be mechanically scanned through the beam. This will allow investigating the interaction between the ion beams of the three microthrusters, the resulting overall beam divergence, the thrust vector position and direction. The complete test set-up consisting of three microthruster modules and the beam scanner will be mounted on one of the removable large end flanges (1.20 m diameter) of the chamber. A special CF 150 UHV flange with the necessary low and high voltage UHV feedthroughs, mounted centrally on the end flange, will allow removing the cluster separately from the chamber.

Data Acquisition System

The cluster will be operated with the present standard laboratory HV power supplies (one power supply for each module). One LV power supply will be sufficient to control the heaters of the three modules.

The following data will be recorded in 0.5 s intervals (2 Hz, i.e. the GOCE sampling rate) using BURR-BROWN PCI-20000 series interface cards and KEITHLEY - LABTECH - NOTEBOOK data acquisition software:

U_1, U_2, U_3	emitter voltage (one for each module)
I_1, I_2, I_3	emitter current (one for each module)
I_c	collector current

Sampling precision of all inputs will be 12 bit. The sampled data are stored on the PC's hard disk. Evaluation and presentation of the data will be performed using Microcal ORIGIN data analysis and technical graphing software for Windows NT. Fig. 7 shows the indium FEEP experimental set-up.

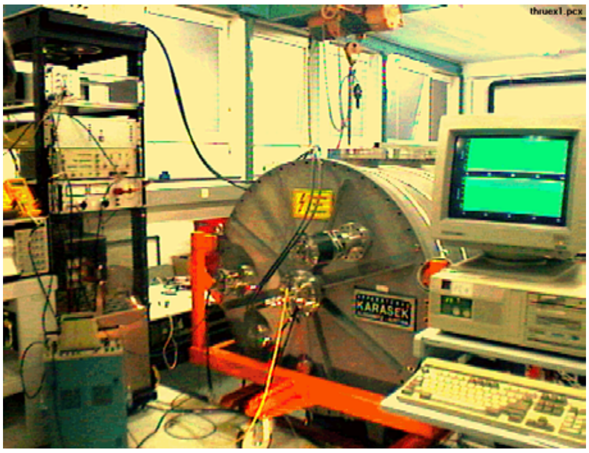

Fig. 7 – View of the indium FEEP experimental set-up: left, power supplies; center, high vacuum chamber, thruster flange; right, data acquisition system.

3.4 Cluster Characterization

Fig. 8 shows the Indium FEEP Cluster, which consists of three flight-representative In-FEEP 100 modules (serial numbers 4, 5, and 7) including the ion emitter, extractor electrode, thermal insulation and heater, each having a distance of approximately 5 cm from each other.

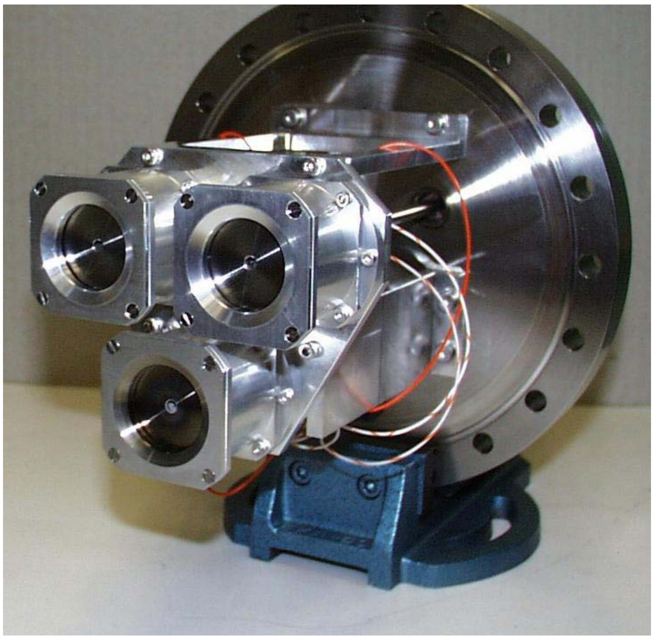

Fig. 8 – Indium FEEP Cluster

Fig. 9 shows the starting phase of the Cluster Test; the three thrusters have been switched on increasing the emitter current (stabilized by standard HEINZINGER HV power supplies) up to 250 µA. From second 1300 to second 1440 they are simultaneously firing at this current level; Fig. 9 also shows the Cluster response in terms of collector current, which corresponds to the total ion current that is actually leaving the Cluster. In this case, it is about 750 µA, that is just the sum of the three emitter currents.

Fig. 10 shows the Cluster response in terms of emitter voltages of the three thrusters. Notice that the voltages corresponding to an emitter current of 250 µA are around 6 kV for the In-FEEP 100 No. 7, 7.4 kV for the In-FEEP 100 No. 4, and more than 8 kV for the In-FEEP No. 5. This is mainly due to differencies in the needle wetting with Indium; the more uniform and thicker the wetting, the better the Indium flow along the needle, the lower the emitter voltage is.

Fig. 10 also shows that the emitter voltages of the three thrusters are not influencing each other. In fact, the In-FEEP No. 4 voltage is not changing when the other two thrusters are switched on (see Fig. 10 @ 1640 s).

Fig. 11 shows the thrusts of the three modules calculated from the emitter currents and the emitter voltages, and the thrust of the Cluster from the collector current and a mean value of the three voltages.

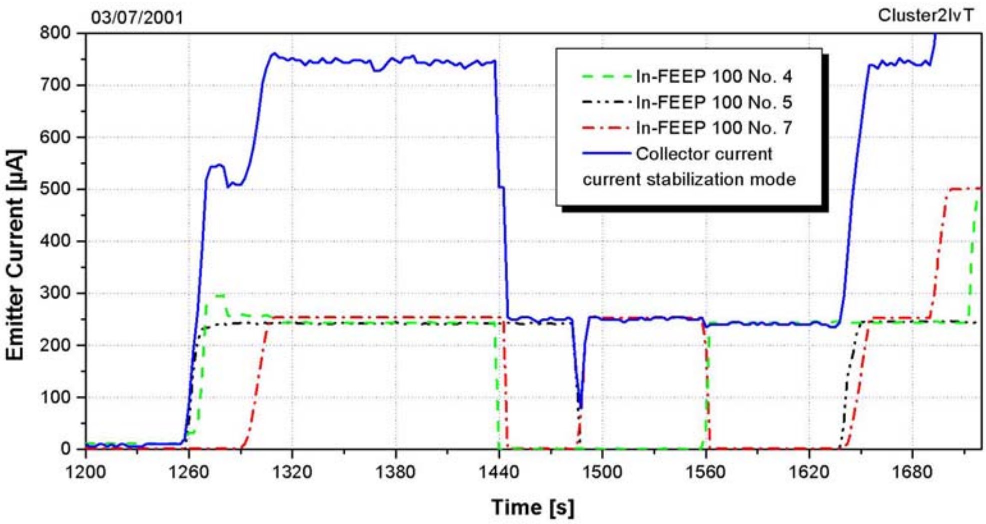

Fig. 9 – Starting phase of the Cluster Test: all three thrusters firing simultaneously at 250 µA

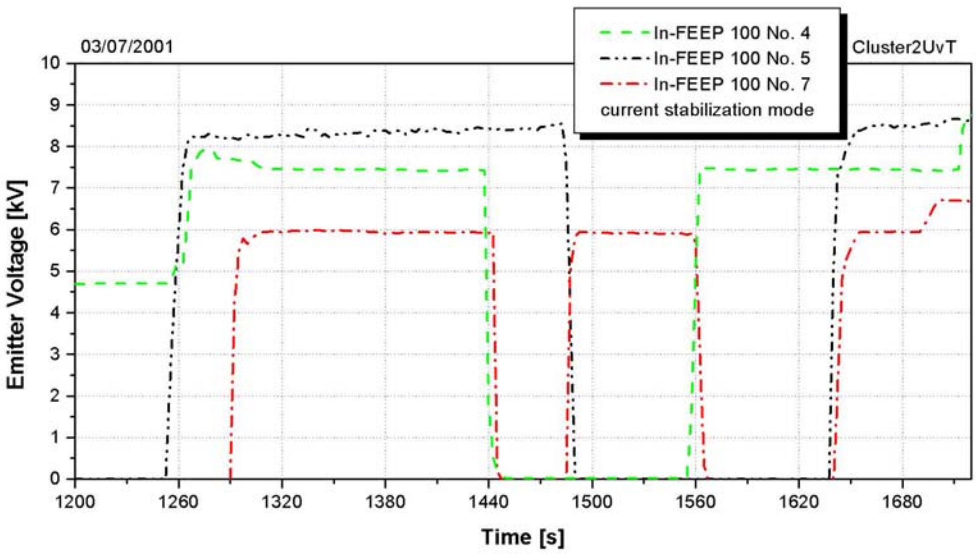

Fig. 10 – Starting phase of the Cluster Test: emitter voltages of the three thrusters.

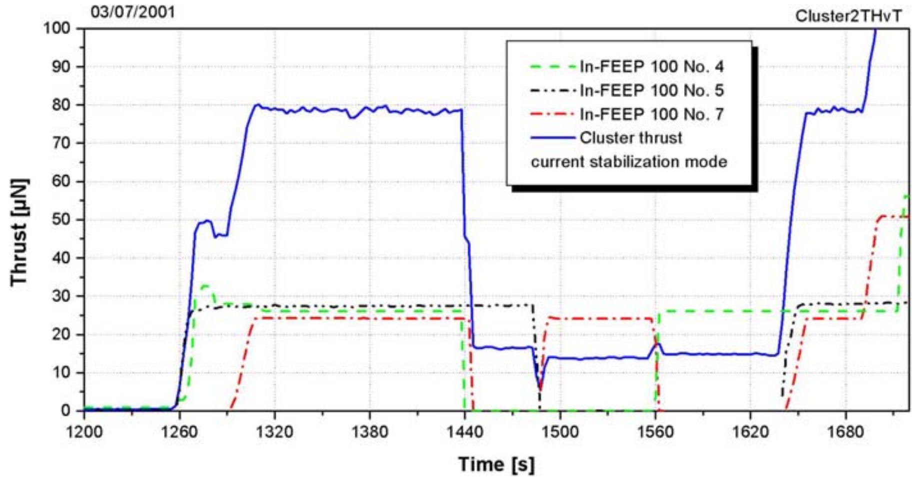

Fig. 11 – Starting phase of the Cluster Test: calculated thrust of each thruster and total thrust of the Cluster

Unfortunately, the In-FEEP 100 No. 5 could not be operated at higher emitter currents than 250 µA, because of a non-proper needle wetting. Hence, it was decided to use the other two thrusters for a preliminary assessment of the Cluster performance at high thrust levels. A new In-FEEP Microthruster (No. 8) is presently under manufacturing and it will be used to replace the faulty one.
Fig. 12 shows the two remaining thrusters firing simultaneously at 600 µA and 800 µA (emitter current). The Cluster response in terms of collector current is also shown in Fig. 12. Fig. 13 shows the corresponding emitter voltages; it is evident the difference between the needle wetting of the two thrusters, as In-FEEP 100 No. 7 only needed about 7.4 kV for 800 µA, while In-FEEP 100 No. 4 needed more than 10 kV for the same emitter current.

Fig. 14 shows the thrusts of the single modules calculated from the emitter currents and the emitter voltages, and the thrust of the Cluster from the collector current and a mean value of the two voltages. In particular, from second 3000 to second 3250 the Cluster thrust was set to the remarkable level of around 170 µN.

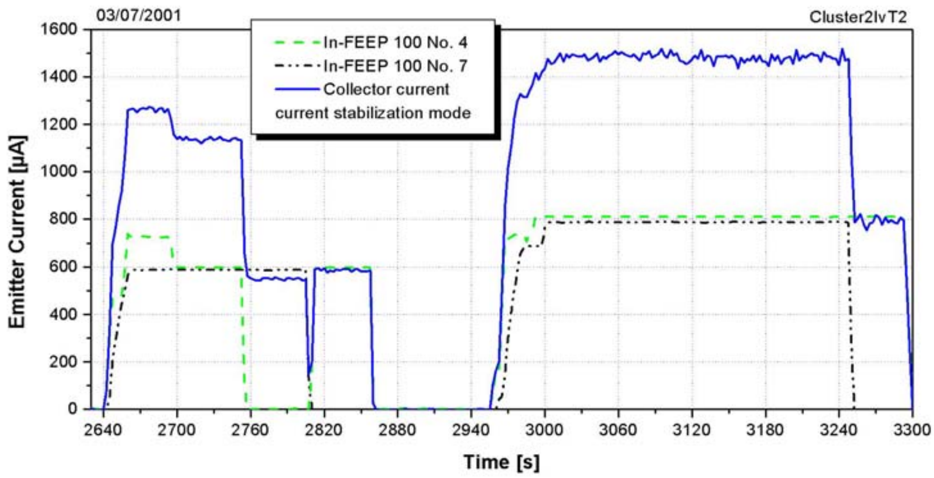

Fig. 12 – Cluster performance at high thrust: two modules firing simultaneously at 600 µA and 800 µA

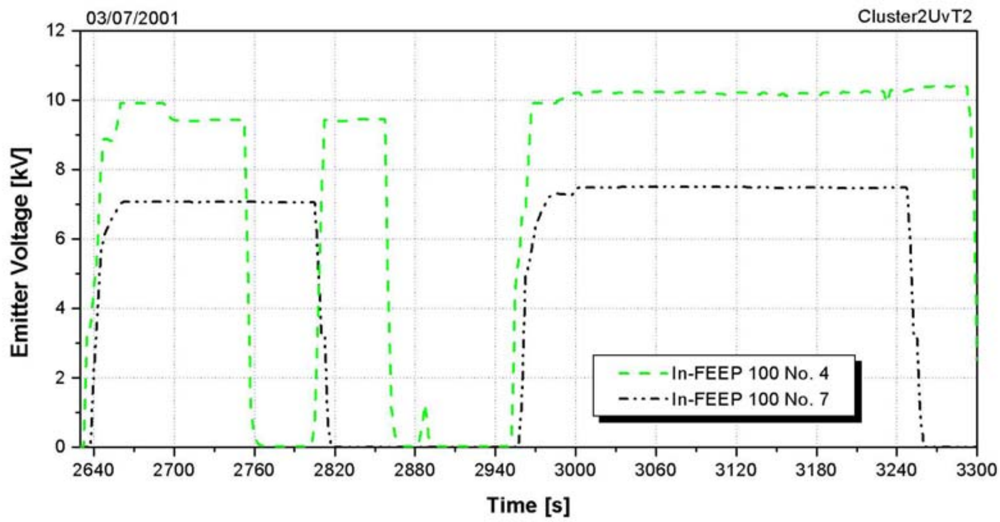

Fig. 13 – Cluster performance at high thrust: emitter voltages.

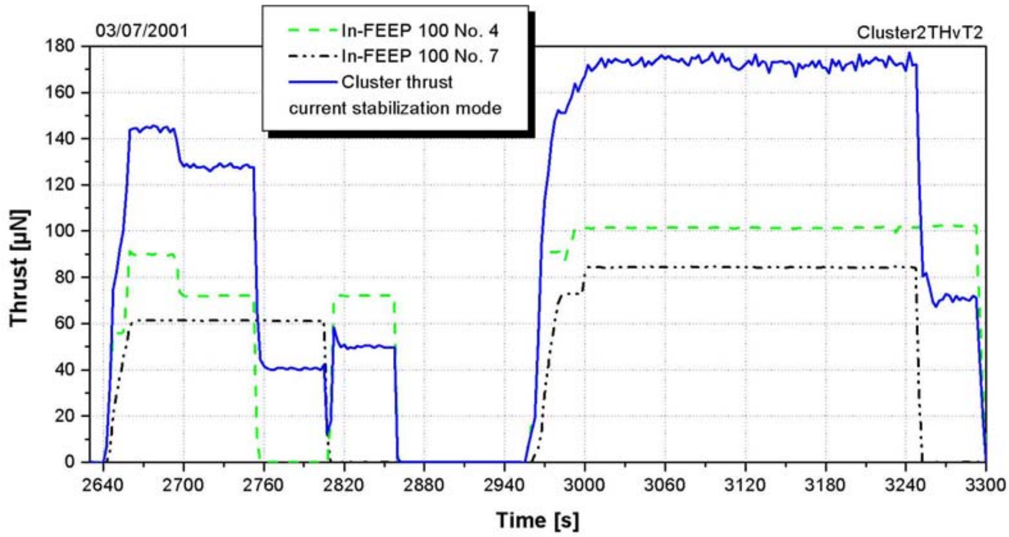

Fig. 14 – Cluster performance at high thrust: calculated thrust of each thruster and total thrust of the Cluster

3.5 Cluster Noise

Fig. 15 shows a test of a single thruster performed in current stabilization mode, that is the emitter current is kept constant by the power supply while the emitter voltage is not controlled. In this case, a slow operating voltage drift may be expected which enhances the low – frequency noise in the computed (and actual) thrust, as shown in Fig. 15. For instance, if the thrust increases by 1% in 100 s and then recovers to the original value, this would mean a 1% noise amplitude at a frequency of 0.01 Hz, a highly undesirable effect considering the GOCE requirements. The same would hold true for abrupt voltage changes and recoveries in that timescale, occasionally observed with FEEP thrusters. Direct thrust stabilization (analog or digital) would detect such drifts or steps on-line and react according to the time constant of the digital or analog regulation circuit respectively.

ARCS has built an analog thrust stabilizer wich allows to operate the Indium FEEP Microthruster at a certain constant thrust with very low noise at low frequencies. Fig. 16 shows that the ARCS Microthruster can even fulfill the very stringent LISA requirements in this operating mode. Unfortunately, during this preliminary assessment of the Cluster performance, the thrust stabilizer was not ready for operating three thrusters simultaneously. Hence, the thrust noise of the Indium FEEP Cluster was investigated in current stabilization mode, which gives us an upper limit to the actual noise.

Fig. 17 shows a comparison between the Cluster thrust noise at 3 µN (each thruster firing at 1 µN), and the noise of a single thruster at 3 µN. The Cluster thrust noise has been derived from the thrust calculated using the collector current, Icoll, and a mean value of the three emitter voltages, Um. Fig. 17 shows that the noise of the Indium FEEP Cluster is only slightly bigger than the noise of a single thruster a the same thrust level.

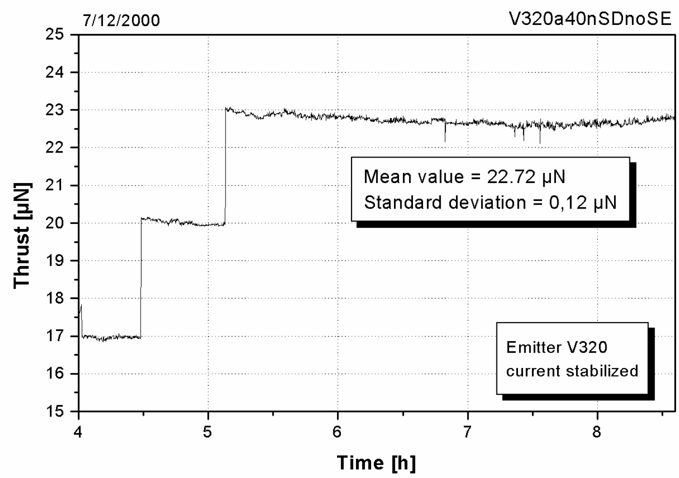

Fig. 15 – Slow drift of thrust in current stabilized mode

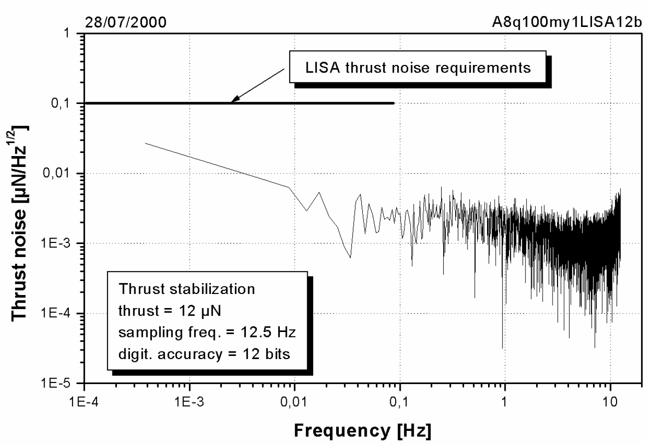

Fig. 16 – Comparison between indium FEEP thrust noise spectral density and LISA requirements.

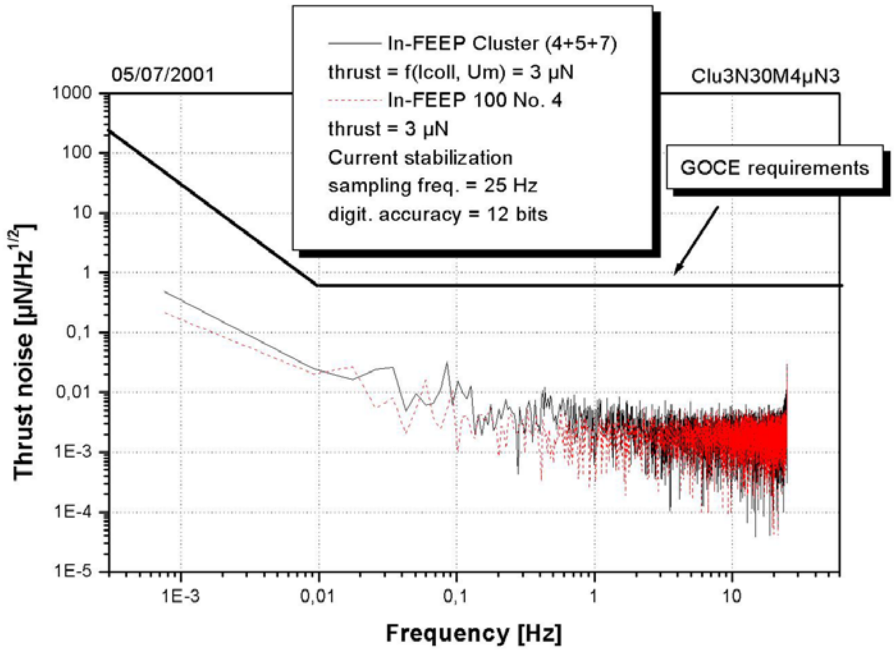

Fig. 17 – Comparison between Cluster noise at 3 µN and single thruster noise at 3 µN

Fig. 18 shows a comparison between the Cluster thrust noise at 9 µN (each thruster firing at 3 µN), and the noise of a single thruster at 9 µN. In this case the noise of the Indium FEEP Cluster is even lower than the noise of a single thruster firing at the same thrust level.

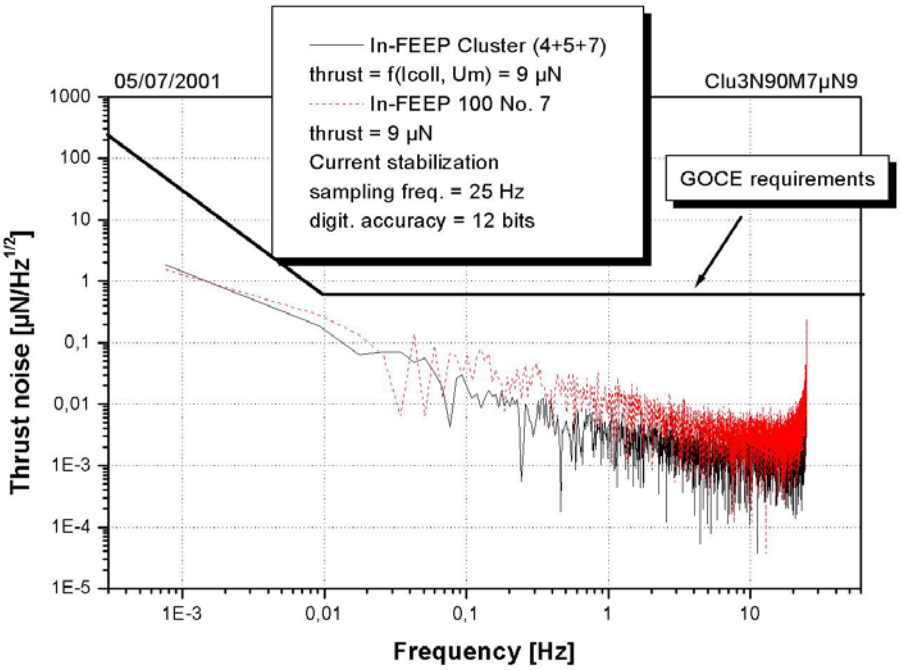

Fig. 18 – Comparison between Cluster noise at 9 µN and single thruster noise at 9 µN

Fig. 19 shows a comparison between the Cluster thrust noise at 62 µN (each thruster firing at about 20 µN), and the noise of a single thruster at 72 µN. The bigger Cluster noise at low frequencies is due to the fact that three thrusters are firing simultaneously; hence, if there is a slow drift in only one of the three emitter voltages, then the resulting low-frequency noise will be enhanced. However, this effect can be smoothed operating the thrusters in thrust stabilization mode. In fact, Fig. 20 shows that in this operating mode the noise of an Indium FEEP Microthruster can be more than one order of magnitude lower than in current stabilization mode.

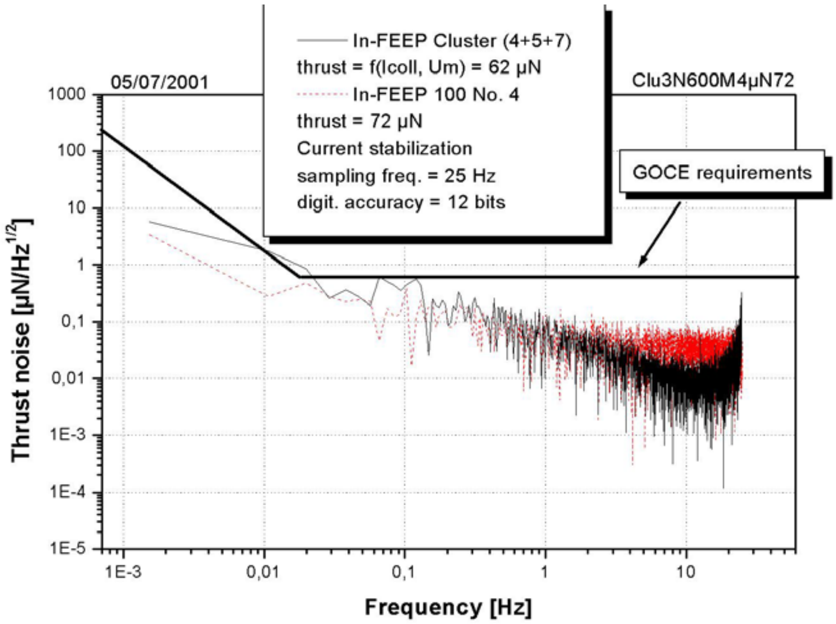

Fig. 19 – Comparison between Cluster noise at 62 µN and single thruster noise at 72 µN

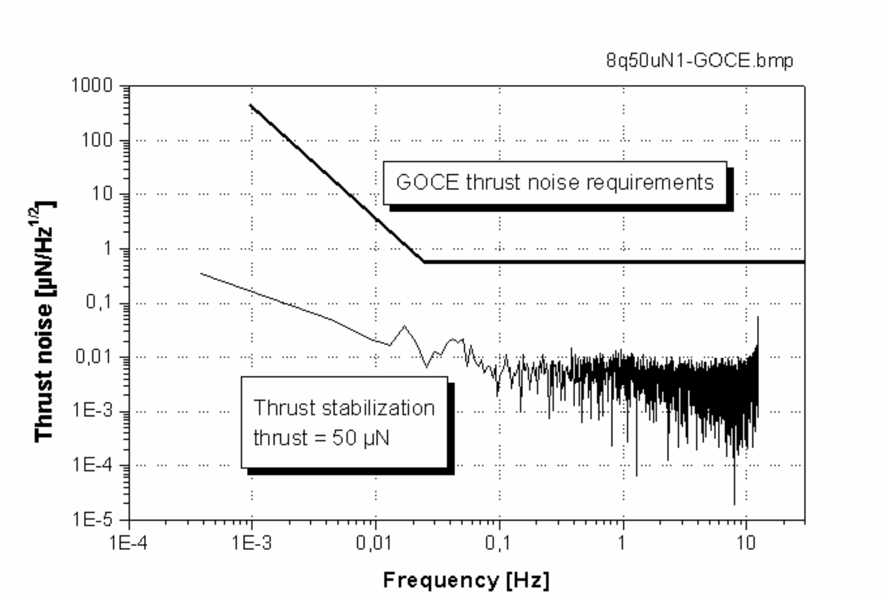

Fig. 20 – Comparison between single thruster noise in thrust stabilization mode and GOCE requirements

3.6 Cluster Beam Diagnostics

Beam profiles were recorded for all emitters operating at the same time as well as each emitter separately. Then the separate profiles were added together and compared with the one obtained for all emitters operating. If both agree, no ion beam interaction is present.

Figure 21 shows multi emitter profiles for three modules operating at 100 µA (total thrust of 30 µN). As it can be clearly seen, the separate profiles add up very well to match the profile recorded for all emitters operating. Therefore, no ion beam interaction is present at this thrust level.

Figure 22 shows the same case for emitters operating at 400 µA (total thrust of 128 µN) with no ion beam present. Unfortunately, higher emission currents for all three modules caused malfunctions in the beam diagnostic electronics. Therefore it was decided only to operate two modules at higher currents. Figure 23 shows two emitters operating at 600 µA (total thrust of 132 µN) and again the separate emitter profiles add up to match the one recorded for both operating at the same time.

In general, no ion beam interaction was found in all multi emitter beam profiles confirming that space charge effects are only limited to the close emitter tip region influencing beam divergence.

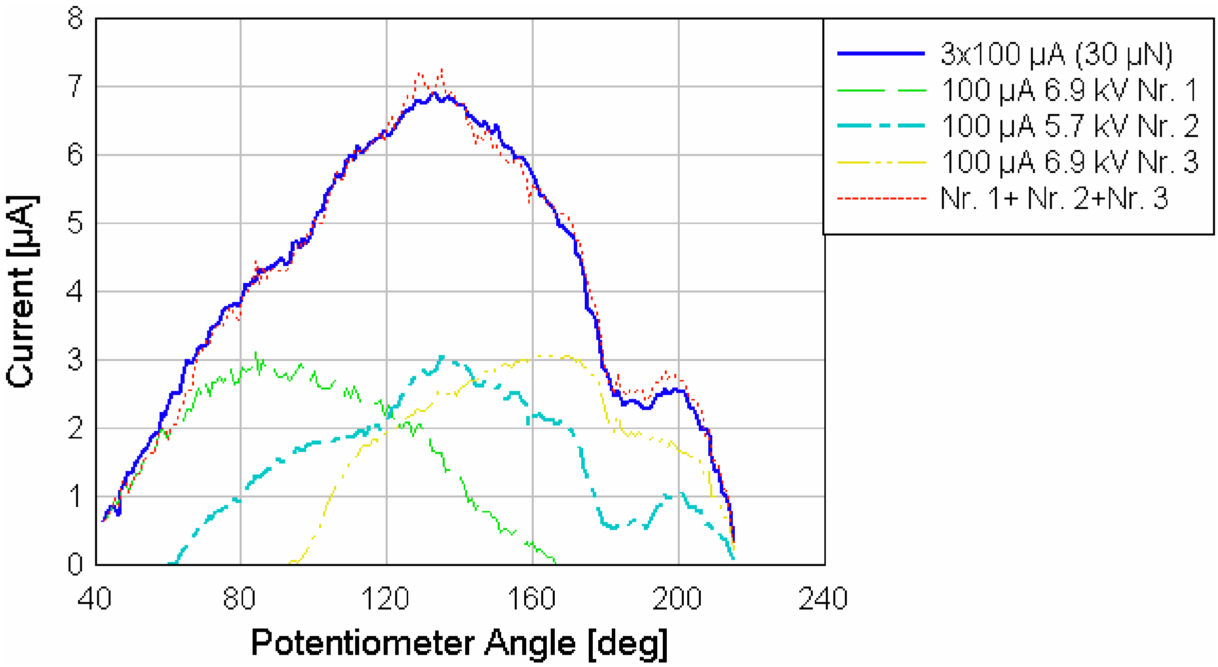

Figure 21 Ion Beam Profile with Wire Probe for 3x100 µA

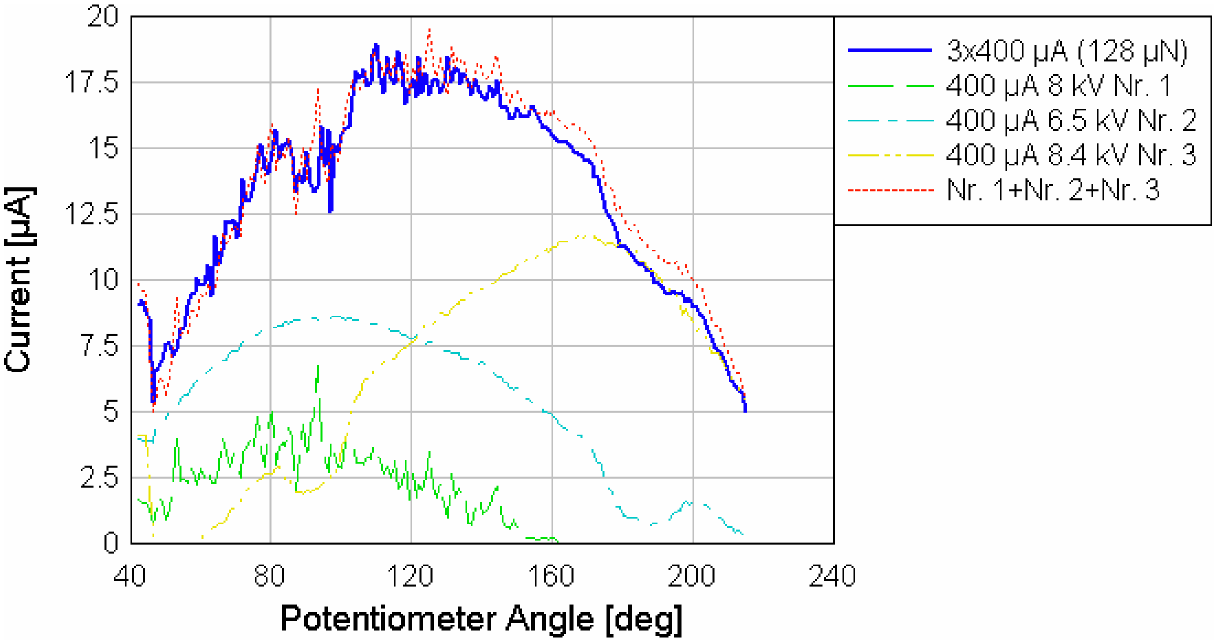

Figure 22 Ion Beam Profile with Wire Probe for 3x400 μA

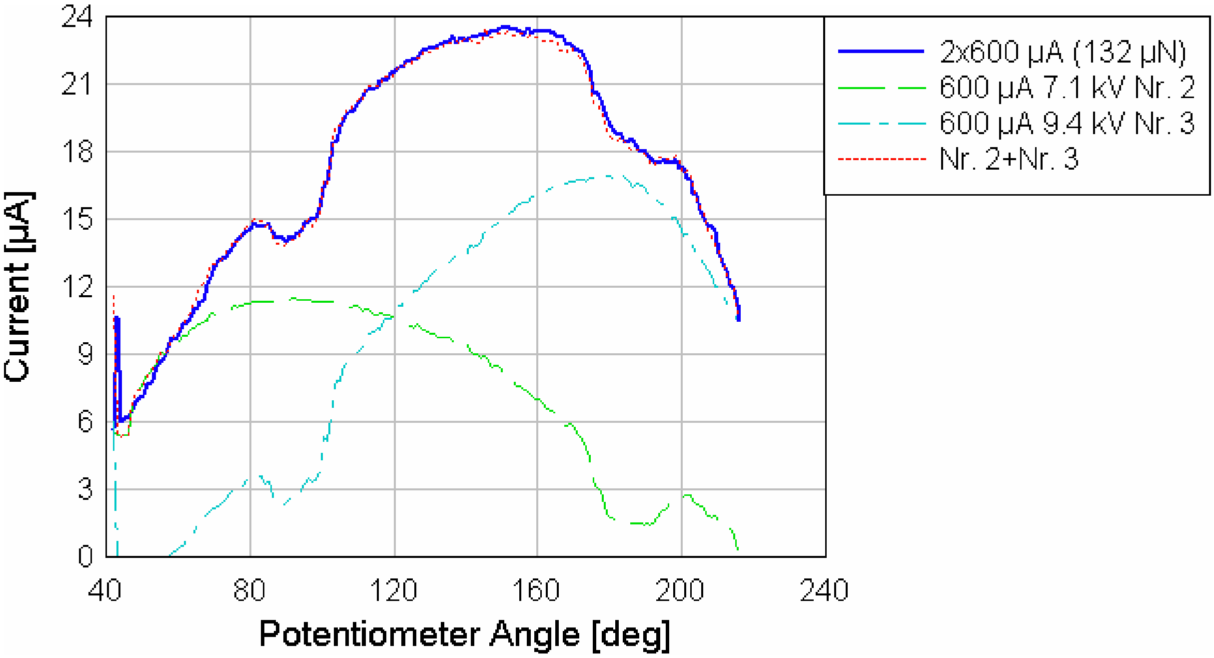

Figure 23 Ion Beam Profile with Wire Probe for 2x600 μA

3.7 Numerical Simulations

Simulation Code Description

A hybrid three-dimensional electrostatic Particle-In-Cell (PIC) code has been developed to study In-FEEP plasmas and spacecraft interactions (Tajmar, M., Rüdenauer, F., and Fehringer, M., "Backflow Contamination of Indium Liquid-Metal Ion Emitters (LMIE): Numerical Simulations", *International Electric Propulsion Conference*, IEPC-99-070, 1999). In this code, all particles (beam ions, charge-exchange ions, sputter neutrals) are treated as computational test particles whereas neutral microdroplets are modeled as a fluid. For a full description of the beam constituents (ions and neutrals) and the numerical mode, the reader is referred to the literature cited.

New virtual instruments were added to the simulation that can model wire probes and Retarding-Potential-Analyzers (RPA) with their real physical dimensions. The simulation was then used to compare with experimental results. Fig. 24 shows an ion beam profile obtained with a wire probe for a beam current of 482 µA and a potential of 9 kV (= 55.6 µN) compared to a virtual probe measurement using the numerical simulation. A secondary electron yield of 3.7 was used in the simulation, a quite reasonable number for ions with energies of approximately 10 keV hitting metallic targets (Chapman, B., "Glow Discharge Processes", John Wiley & Sons, 1980, pp. 87). The agreement is very good and verified our simulation approach.

Cluster Simulation

A numerical simulation was carried out for the cluster configuration of three emitters as described in the previous chapter. All emitters were set to I=600 µA and U=10 kV, the simulation domain was 0.1x0.1x0.1 m and a total number of 150,000 particles were used. The ambient environment was set vacuum conditions in order to study the worst case scenario with no additional electrons that can provide neutralization.

Fig. 25 shows the ion density and potential distribution in a 3D view. Both plots show that the beam becomes quickly very homogeneous. In the main interaction area in the middle of the simulation domain (Z=0.5 m) the potential is around 200 Volts. This is very small compared to ion energies of 10 keV. Also the homogeneous distribution suggests no significant radial electric fields which can cause the beams to repel or attract each other.

The ion densities are shown in greater detail in Fig. 26. Comparing the single needle emission with the distribution of two needle emitters close to each other, the latter looks like a superposition of two single ones. Also this suggests no interaction between the ion beams. Also the potentials along emission in Z-direction shown in Fig. 27 indicate no difference between single emission and two emitters operating closely together.

A virtual Retarding-Potential-Analyzer was put in the middle of the simulation domain to evaluate energies of the ion beam particles. Fig. 28 shows a peak at the primary energy due to the emission from the needle, a broadening of +/- 200 Volts due to possible ion beam interactions and a higher energy tail due to a Maxwell temperature distribution on top of the primary acceleration energy. This 200 V is consistent with the potential plots and, as discussed previously, only cause minor interactions with the ion beam. These results were obtained for vacuum emission and represent a worst case scenario that can not be obtained from ground testing.

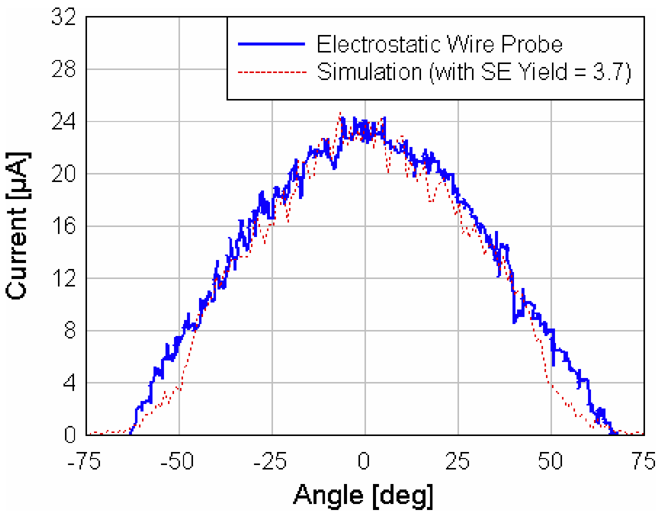

Fig. 24 Comparison of Wire Probe Beam Profile and Virtual Probe in Particle Simulation

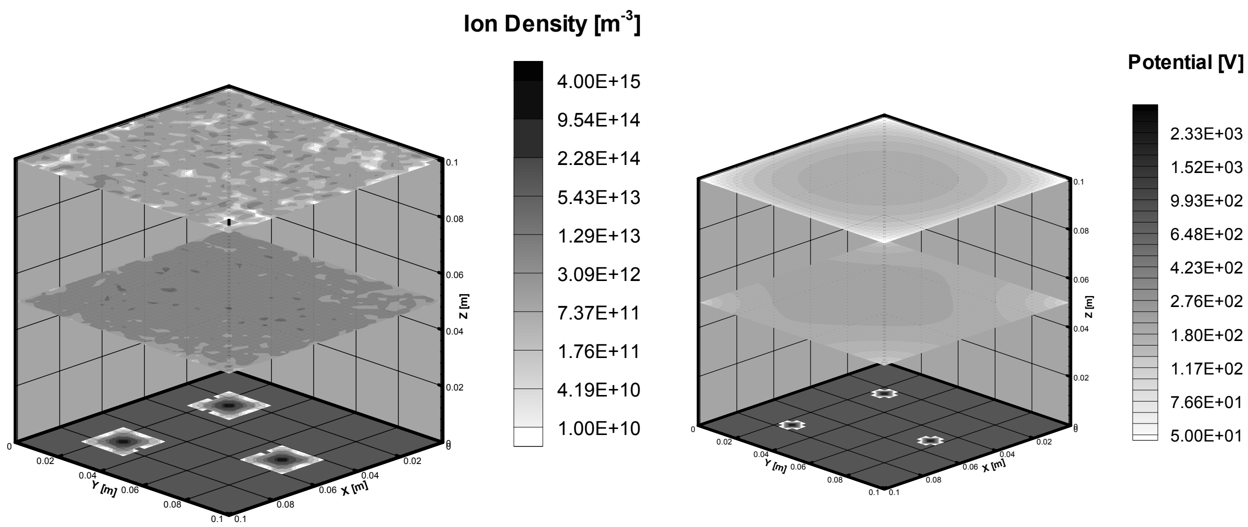

Fig. 25 3D Ion Density and Potential Distribution

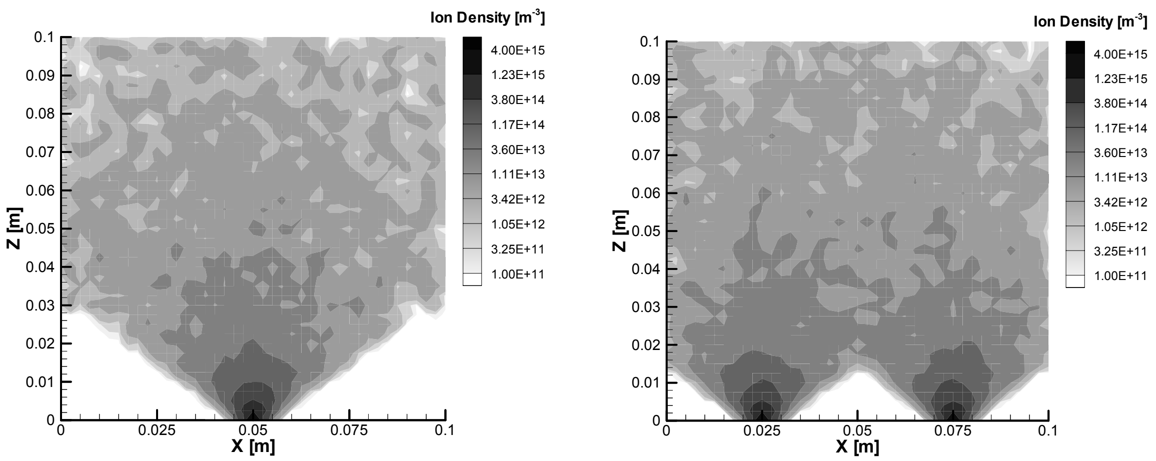

Fig. 26 Ion Density crossing the 3D View at Y=0.25 and Y=0.75 m

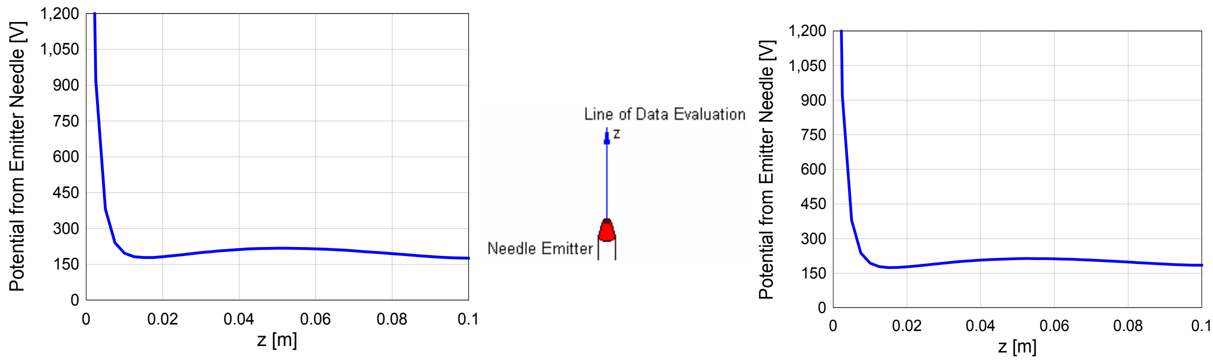

Fig. 27 Potentials from Needle Locations in Z-Direction (Left from Y=0.25 m, Right from Y=0.75 m)

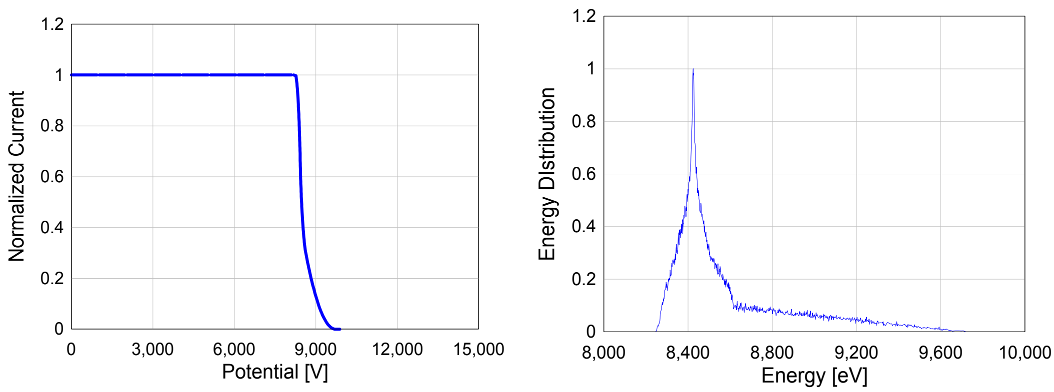

Fig. 28 Virtual Retarding-Potential-Analyser in the Middle of the Simulation Domain

Conclusion

In-FEEP ion beam profiles were obtained for a variety of thrust values ranging from 0.49 up to 115.5 μN. The beam shape was found to be close to a cosine in low thrust levels and resembled a Gaussian distribution at high thrust levels. Data processing of the obtained profiles to evaluate the thrust correction factor which is in close agreement to direct thrust measurements. Thrust vector angle and beam divergence were within the expected ranges.

A multi-emitter configuration was tested and the ion beam profiles showed no ion beam interaction. Numerical simulations based on a 3D Particle-In-Cell (PIC) code, successfully tested against experimental measurements, verified this result even for a vacuum environment with no ambient electrons that can provide neutralization.